ICARUS **125,** 416–439 (1997)
ARTICLE NO. IS965628

The Oxidation State of the Lower Atmosphere and Surface of Venus

BRUCE FEGLEY, JR.

Planetary Chemistry Laboratory, Department of Earth and Planetary Sciences, and McDonnell Center for the Space Sciences, Washington University, One Brookings Drive, St. Louis, Missouri 63130-4899
E-mail: bfegley@levee.wustl.edu

MIKHAIL YU. ZOLOTOV

Vernadsky Institute, Russian Academy of Sciences, Moscow, Russia

AND

KATHARINA LODDERS

Planetary Chemistry Laboratory, Department of Earth and Planetary Sciences, Washington University, One Brookings Drive, St. Louis, Missouri 63130-4899

Received May 20, 1996; revised August 18, 1996

We present a comprehensive study of the redox state of the lower atmosphere and surface of Venus. This study constrains the CO concentration and oxygen fugacity at the surface of Venus. It incorporates: (1) gas phase thermochemical equilibrium and kinetic calculations to model the chemistry of the near-surface atmosphere, (2) a reanalysis of the thermodynamics of the CONTRAST experiment on the Venera 13 and 14 landers, (3) carefully selected thermodynamic data to model the stability of magnetite and hematite on the surface of Venus, and (4) the Venera 9 and 10 lander spectral reflectance data presented by Pieters *et al.* (1986, *Science* 234, 1379–1383). The results of our work predict that: (1) the CO concentration at 0 km (735 K) is in the range of 3–20 parts per million by volume, (2) the oxygen fugacity (fO_2) at 0 km is in the range of $10^{-21.7}$ to $10^{-20.0}$ bars, (3) the fO_2 of the atmosphere at 0 km is indistinguishable, within the uncertainties of the thermodynamic data, from the magnetite–hematite phase boundary, (4) gas phase thermochemical equilibrium is reached only, if at all, in the lowest levels of the atmosphere below about 0.7 km (730 K), (5) a disequilibrium region which is more oxidizing than predicted by thermochemical equilibrium exists at higher elevations, and (6) hematite forms at higher elevations due to the more oxidizing conditions in the disequilibrium region. Finally, we suggest experimental, observational, and theoretical studies which can be used to test our predictions and to provide a foundation for the design of experiments on future spacecraft lander missions to Venus.

INTRODUCTION

The oxidation (redox) state of Venus' near-surface atmosphere controls the abundances of minor and trace gases and the chemical weathering of primary minerals to secondary minerals (i.e., soil) on the surface. Physical properties such as the spectral reflectance, dielectric constant, electrical conductivity, magnetic susceptibility of rock and soil, and the loss of water from Venus over geologic time (via oxidation of the surface and hydrogen escape to space) are also influenced by the redox state of the atmosphere. The relative concentrations of oxidized versus reduced carbon, sulfur, and hydrogen gases, resulting from the net thermochemical reactions

$$2CO + O_2 = 2CO_2 \quad (1)$$

$$CH_4 + 2O_2 = CO_2 + 2H_2O \quad (2)$$

$$OCS + O_2 = SO_2 + CO \quad (3)$$

$$H_2S + 1.5O_2 = SO_2 + H_2O \quad (4)$$

$$S_2 + 2O_2 = 2SO_2 \quad (5)$$

$$2H_2 + O_2 = 2H_2O, \quad (6)$$

are dependent upon the oxygen fugacity (fO_2) of the near-surface atmosphere. Sufficiently low oxygen fugacities, favor CO, CH_4, OCS, H_2S, S_2, and H_2 at the expense of CO_2, SO_2, and H_2O, while higher fO_2 leads to the opposite situation (e.g., see Fig. 1).

Likewise, the stability of Fe^{2+}- and Fe^{3+}-bearing minerals and the Fe^{2+}/Fe^{3+} ratio of the surface (which are related to the ability of the surface to act as an oxygen sink during water loss) are also influenced by the oxygen fugacity. This can be seen from the exemplary gas-solid reactions

0019-1035/97 $25.00

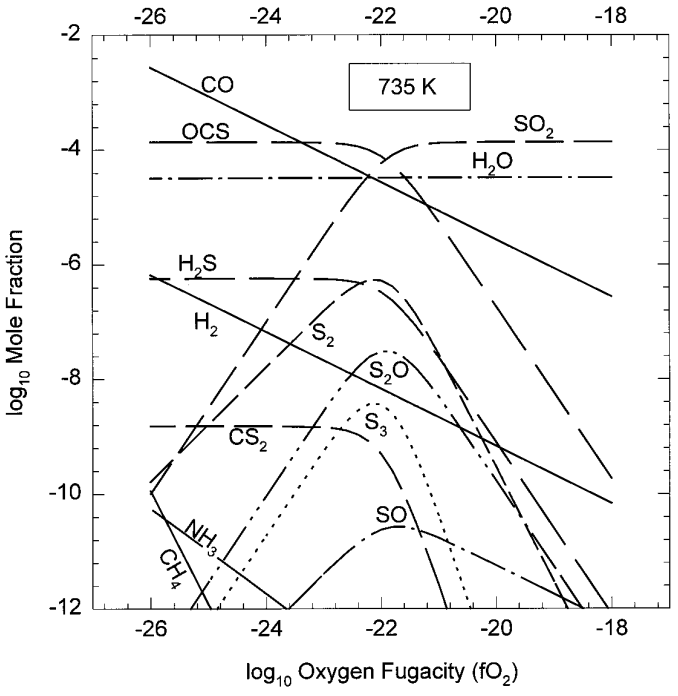

FIG. 1. Calculated equilibrium gas mole fractions as a function of oxygen fugacity at 735.3 K (0 km). Spectroscopic observations or *in situ* measurements of SO_2, OCS, CO, H_2S, S_2, CH_4, NH_3, and H_2 can constrain the redox state of the near-surface atmosphere of Venus because the concentrations of these gases are sensitive functions of the oxygen fugacity.

$$4Fe_3O_4 \text{ (magnetite)} + O_2 = 6Fe_2O_3 \text{ (hematite)} \quad (7)$$

$$4FeSiO_3 \text{ (ferrosilite in pyroxene)} + O_2 = 2Fe_2O_3 \text{ (hematite)} + 4SiO_2 \text{ (silica)} \quad (8)$$

$$2Fe_2SiO_4 \text{ (fayalite in olivine)} + O_2 = 2Fe_2O_3 \text{ (hematite)} + 2SiO_2 \text{ (silica)}. \quad (9)$$

Reducing conditions favor Fe^{2+}-bearing pyroxene and olivine and large Fe^{2+}/Fe^{3+} ratios, while oxidizing conditions favor hematite, other Fe^{3+}-bearing phases, and small Fe^{2+}/Fe^{3+} ratios.

During the past 30 years several attempts have been made to calculate and measure the oxygen fugacity of Venus' lower atmosphere from Earth-based remote sensing and spacecraft observations. Mueller (1964) used Kuiper's (1952) upper limit of $CO/CO_2 \leq 10^{-3}$ to deduce that "$P_{O2} \geq 10^{-27.1}$ atm at 700° K, which is in the center of the magnetite field." Later, after the discovery of CO on Venus by Connes *et al.* (1968), Lewis (1970) used the observed CO abundance at the cloud tops and reaction (1) to calculate $fO_2 = 10^{-23.10}$ bars at 747 K on the surface of Venus. Lewis (1970) also found that magnetite was the stable iron oxide under these conditions and that OCS and H_2S were more abundant than SO_2 (a molar $(OCS + H_2S)/SO_2$ ratio ~165).

After the Pioneer Venus (PV) and Venera 11/12 missions analyzed the venusian atmosphere down to 22 km altitude, Lewis and Kreimendahl (1980) revisited the question of the oxidation state of the atmosphere and surface. They used upper limits on the abundances of CH_4 and H_2 to set lower limits of $fO_2 > 10^{-25.9}$ bars from reaction (2) and $fO_2 > 10^{-23.5}$ bars from reaction (6) at the surface of Venus. With slight modifications due to improved knowledge of the temperature and water vapor abundance at the surface of Venus, these lower limits are still valid today.

Conversely, by considering reactions (3) and (4), Lewis and Kreimendahl (1980) attempted to set upper limits on the fO_2 at the surface of Venus. Based upon the preliminary results from the PV mass spectrometer experiment (Hoffman *et al.* 1979), Lewis and Kreimendahl (1980) concluded that the oxidation state of the surface was controlled by the pyrite–calcite–anhydrite–wüstite (PCAW) buffer,

$$2FeS_2 \text{ (pyrite)} + 2CaCO_3 \text{ (calcite)} + 7O_2 = 2CaSO_4 \text{ (anhydrite)} + \text{'FeO' (wüstite)} + 2CO_2, \quad (10)$$

and that $\log_{10} fO_2 = -22.6^{+0.1}_{-0.4}$ at 750 K. However, their conclusion rested upon the assumption that "... the dominance of OCS + H_2S over SO_2, first postulated by Lewis (1969) and confirmed by Pioneer Venus, requires $P_{O2} \leq 10^{-21.4}$" (Lewis and Kreimendahl 1980). As reviewed by Von Zahn *et al.* (1983), the final results from the PV and Venera 11/12 missions show that SO_2 is the dominant sulfur gas, at least above 22 km. Lewis and Kreimendahl (1980) also opined that "It is clear that the surface of Venus does not lie in or near the hematite (Fe_2O_3) stability field."

Barsukov *et al.* (1982) used the Venera 11/12 and PV results to calculate $\log_{10} fO_2 \sim -21$ at 750 K and proposed that the pyrite–calcite–anhydrite–magnetite buffer,

$$3FeS_2 + 6CaCO_3 + 11O_2 = 6CaSO_4 + Fe_3O_4 + 6CO_2, \quad (11)$$

controls the redox state of Venus' surface and lower atmosphere. They also predicted that magnetite, and not hematite, is stable on the surface.

Several attempts have also been made to measure directly O_2 in the middle atmosphere of Venus. Assuming that O_2 is uniformly mixed, the Earth-based spectroscopic observations of Trauger and Lunine (1983) set an upper limit of <0.3 ppm O_2 at the cloud tops. However, measurements by the Pioneer Venus (Oyama *et al.* 1980) and Venera 13/14 (Mukhin *et al.* 1983) gas chromatographs reported much larger O_2 levels (e.g., 44 ± 25 ppm at 52 km and 16 ± 7 ppm at 42 km from PV and 18 ± 4 ppm at 35–58 km from Venera 13/14) in the subcloud atmosphere. These data are probably unreliable (Von Zahn *et al.* 1983; Krasnopolsky 1986) and are contradicted by the upper limit of <20 ppm O_2 below 42 km from the Venera 11/12

gas chromatograph (Gel'man *et al.* 1979), the upper limit of <50 ppm O_2 below 60 km from the Venera 11/12 spectrophotometer experiment (Moroz 1981), and the spectroscopic upper limit of Trauger and Lunine (1983). In addition, all these data are for relatively high altitudes (>20 km) in the atmosphere of Venus. Thus, neither the reported detections of O_2 nor the upper limits on O_2 can be used to deduce the oxidation state of the lower atmosphere (<20 km) and surface.

The theoretical deductions that magnetite was stable on the surface of Venus and that the oxygen fugacity at the surface was less than that at the magnetite-hematite phase boundary were apparently supported by the results of the CONTRAST color change experiment on the Venera 13/14 landers (Florensky *et al.* 1983a,b). The CONTRAST experiment qualitatively measured the CO content at the surface of Venus from the color change from white to black for the reaction

$$Na_4V_2O_7 + 2CO = V_2O_3 + 2Na_2CO_3 \quad (12)$$

or from white to dark blue for the reaction

$$Na_4V_2O_7 + CO + CO_2 = V_2O_4 + 2Na_2CO_3 \quad (13)$$

for asbestos paper impregnated with sodium pyrovanadate ($Na_4V_2O_7$). Reactions (12) and (13) both give a color change if the CO partial pressure is at, or above, the equilibrium value. Thus, the CONTRAST experiment constrains the lower limit for the CO concentration at the Venera 13/14 landing sites. Florensky *et al.* (1983a,b) reported that the observed darkening of the asbestos paper gave ≥10 ppm for CO, and using reaction (1), $fO_2 \leq 10^{-21}$ bars, which is inside the magnetite stability field at Venus surface temperatures.

The (qualitative) CONTRAST experiment may have been influenced by dust and soil thrown up by the spacecraft landing. Figure 2 of Florensky *et al.* (1983a) shows that the soil-free and soil-covered portions of the CONTRAST indicator on Venera 13 could be distinguished. Recent image processing by Yu. M. Gektin (personal communication to M. Yu. Zolotov, 1996) shows that all the soil-free areas of the CONTRAST indicators are covered by dust. Even so, the low albedo of these areas indicates vanadium oxide formation and hence reducing conditions.

It was therefore somewhat surprising when Pieters *et al.* (1986) presented evidence that Fe^{3+}-bearing minerals, such as hematite, are present on the surface of Venus. Pieters *et al.* (1986) used a combination of the Venera 9/10 wide angle photometer measurements (Ekonomov *et al.* 1980) and the Venera 13/14 color images (Golovin *et al.* 1983) to derive the spectral reflectance of the surface from 0.54 to 1.0 μm. At visible wavelengths either Fe^{2+}- or Fe^{3+}-bearing phases matched the observations. However, a high reflectance in the near-IR region apparently required Fe^{3+}-bearing minerals such as hematite. However, as seen above, theoretical modeling and the CONTRAST experiment apparently predicted that magnetite was present instead of hematite.

Thus, until recently, it appeared that the two indirect observations of the redox state of the near-surface atmosphere and surface of Venus disagreed with one another. Furthermore, thermodynamic calculations done over a 30-year period predicted that magnetite, and not hematite, was present on Venus. However, several recent developments led us to revisit these issues.

First, the discovery of spectral ''windows'' in the near IR region allows Earth-based observations of Venus' lower atmosphere down to the surface. Earth-based and Galileo spacecraft IR observations in these spectral windows have provided much new information on the chemical composition of Venus' atmosphere (e.g., Bézard *et al.* 1990, 1993, DeBergh *et al.* 1995, Drossart *et al.* 1993, Meadows and Crisp 1996, Pollack *et al.* 1993). In addition, recently published results from the Venera 11/12 and Vega 1/2 missions give data on the CO and SO_2 abundances down to 12 km altitude in Venus' atmosphere (Bertaux *et al.* 1996, Marov *et al.* 1989).

Second, new experimental data from O'Neill (1988) and Hemingway (1990) suggest that the magnetite–hematite (MH) boundary is more reducing than given by tabulated thermodynamic data (Chase *et al.* 1985, Stull and Prophet 1971, Robie and Waldbaum 1968, Robie *et al.* 1979), which were used in prior models of the redox state of Venus' surface and lower atmosphere. In addition, using studies of iron oxides in terrestrial rocks as a guide (Lindsley 1991; Ghiorso and Sack 1991), Zolotov (1994a) suggested that hematite solid solutions with ilmenite ($FeTiO_3$) and geikielite ($MgTiO_3$) are stable to lower fO_2 than pure hematite. However, thermodynamic data for magnetite and hematite in various evaluations scatter a great deal and the fO_2 of the MH boundary varies by over three orders of magnitude at Venus surface temperatures.

Third, while reviewing the results of the CONTRAST experiment, Zolotov (1995) found that the thermodynamic data from Naumov *et al.* (1971) used by Florensky *et al.* (1983a,b) were incomplete. He recalculated the fO_2 for the CONTRAST experiment and found an upper limit of $\leq 10^{-19.7}$ bars for the fO_2, corresponding to ≥2.5 ppm CO.

Last, Fegley *et al.* (1995a,b) observed production of hematite and Fe^{3+}-bearing pyroxene in CO–CO_2 and CO–SO_2–CO_2 gas mixtures with compositions falling inside the magnetite stability field. These experiments indicate that CO_2, CO, and SO_2 may not chemically equilibrate at Venus surface temperatures (about 660 to 740 K). This led Fegley *et al.* (1995b) to propose that the red color observed by Pieters *et al.* (1986) is due to subaerial oxidation of Fe^{2+}-bearing basalt to hematite and other Fe^{3+}-bearing phases

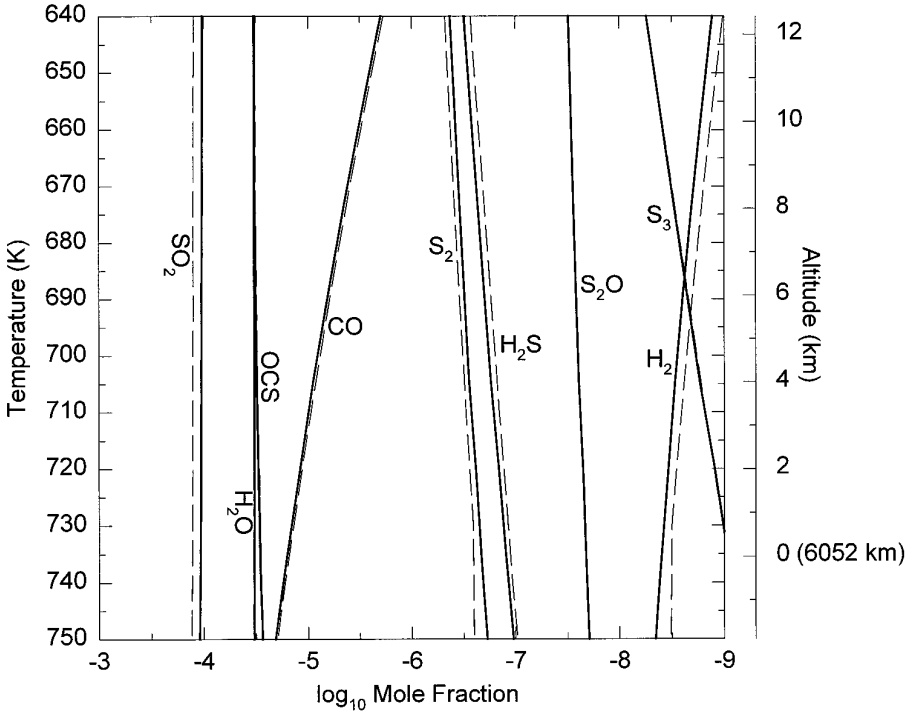

FIG. 2. Calculated equilibrium abundances of C–O–N–S–H gases (other than CO_2 and N_2) in the lower atmosphere of Venus. Gases with mole fractions of at least 1 part per billion by volume (ppbv) are shown. The solid lines are the Washington University calculations using data from Gurvich *et al.* (1989–1994) and the dashed lines are the Vernadsky Institute calculations. The temperature, pressure profile used is given in Table I. Gas abundances at 740 K (corresponding to the modal planetary radius of 6051.4 km) and 735.3 K (corresponding to 6052.0 km radius) are listed in Table IV. Here and in subsequent figures the zero level for the altitude scale is 6052.0 km radius, from the VIRA model (Seiff *et al.* 1986).

on the surface of Venus. This explanation and Zolotov's (1994a) suggestion that hematite solid solutions are more stable than pure hematite are two alternatives that predict hematite and other Fe^{3+}-bearing phases on the surface of Venus. In the next sections we use these new data, experiments, and models to reexamine the following key questions:

First, what is the redox state of the atmosphere at the surface of Venus and how does it vary as a function of altitude? The altitude range over which atmospheric gases equilibrate with each other is related to this question.

Second, how does the redox state of the near-surface atmosphere affect the abundances of minor and trace gases? A related question is how Earth-based spectroscopic observations of the near-surface atmosphere can be used to constrain the atmospheric fO_2 and redox state.

Third, is either magnetite or hematite stable on the surface of Venus, or does the surface lie right on the MH phase boundary? Related issues include the selection of the best available thermodynamic data for magnetite and hematite, the constraints obtained from the CONTRAST experiment on the Venera 13 and 14 landers, and the constraints from the Venera 9 and 10 spectral reflectance data indicating the presence of hematite on the surface of Venus.

ATMOSPHERIC STRUCTURE AND COMPOSITION MODELS

We made independent sets of multicomponent gas phase thermochemical equilibrium calculations at the Vernadsky Institute (VI) and at Washington University (WU). Both sets of calculations used the Venus International Reference Atmosphere (VIRA) model (Seiff *et al.* 1986) for the lower atmosphere of Venus (see Table I). Slightly different chemical composition models, summarized in Table II, were used in the two sets of calculations. The two adopted models are based on our assessments of the spacecraft and Earth-based atmospheric composition measurements (Zolotov 1995, Fegley *et al.* 1996), which we briefly review below.

Carbon dioxide and nitrogen. Both sets of calculations used the CO_2 and N_2 mole fractions of 96.5% and 3.5% recommended by Von Zahn *et al.* (1983).

Sulfur dioxide. Both sets of calculations used an SO_2 abundance of 130 ppm based on the 130 ± 35 ppm SO_2 observed by the Venera 11/12 gas chromatograph (Gel'man *et al.* 1979) at altitudes of 42 km and below and on the Earth-based IR observations of Bézard *et al.* (1993) who reported 130 ± 40 ppm SO_2 in the 35- to 45-km range.

TABLE I
Altitudes, Pressures, and Temperatures in the Near-Surface Atmosphere of Venus[a,b]

Altitude (km)	Temperature (K)	Pressure (Bars)
-2	750.8	104.7
0	735.3	92.10
2	720.2	81.09
4	704.6	71.20
6	688.8	62.35
8	673.6	54.44
10	658.2	47.39
12	643.2	41.12
14	628.1	35.57

[a] Seiff *et al.* (1986).
[b] Relative to 6052 km radius (0 km level). At the modal, median, and mean planetary radii of 6051.4, 6051.6, and 6051.8 km (Ford and Pettengill 1992) the temperature and pressure are 740 K and 95.6 bars, 738.4 K and 94.5 bars, and 736.8 K and 93.3 bars, respectively.

The adopted SO_2 mole fraction is also consistent with the Pollack *et al.* (1993) value of 180 ± 70 ppm SO_2 at 42 km, but is slightly lower than the 185 ± 43 ppm reported by the PV gas chromatograph at 22 km (Oyama *et al.* 1980).

The results of the UV spectroscopy experiment on the Vega 1/2 spacecraft were recently reanalyzed to give SO_2 abundances as a function of altitude in Venus' lower atmosphere (Bertaux *et al.* 1996). At 42 km, the Vega 1 probe found 125 ppm SO_2 while the Vega 2 probe found 140 ppm. These values are about the same as the SO_2 abundances found in the same altitude region by the Venera 11/12 probes, the PV probe, and the Earth-based IR observations. At lower altitudes, where no other data are available, Bertaux *et al.* (1996) reported lower SO_2 abundances of 20–25 ppm at 12 km.

TABLE II
Starting Compositions for Chemical Equilibrium Calculations (C–O–N–S–H System)[a]

Gas	Vernadsky Institute	Washington University
CO_2	96.5%	96.5%
N_2	3.5%	3.5%
SO_2	130 ppm	130 ppm
H_2O	30 ppm	30 ppm
CO	17 ppm	23 ppm
OCS	28 ppm	4.4 ppm
H_2S	0.1 ppm	3 ppm
S_2	0.2 ppm	---

[a] The starting compositions are discussed in the text. The Washington University model also includes 0.5 ppm HCl and 5 ppb HF.

Water vapor. Both sets of calculations used 30 ppm H_2O. Within uncertainties, this is the same as that found from Earth-based IR and Galileo spacecraft observations of the lower atmosphere of Venus (e.g., Drossart *et al.* 1993, Pollack *et al.* 1993, DeBergh *et al.* 1995, Meadows and Crisp 1996) and from analyses by the PV mass spectrometer (Donahue and Hodges 1993).

Carbon monoxide. The calculations done at VI used 17 ppm CO based on the 17 ± 1 ppm CO reported by the Venera 11/12 gas chromatograph at 12 km altitude (Gel'man *et al.* 1979, Marov *et al.* 1989). The calculations done at WU used 23 ppm CO based on IR observations showing 23 ± 5 ppm CO at 36 km altitude (Pollack *et al.* 1993) and on the 20 ± 3 ppm CO found by the PV gas chromatograph at 22 km (Oyama *et al.* 1980).

Reduced sulfur gases. The calculations done at VI used 28 ppm OCS, the value calculated near the surface of Venus by Krasnopolsky and Pollack (1994) from their kinetic modeling. A value of 4.4 ppm OCS was used at WU, based on the IR observations showing 4.4 ± 1 ppm OCS at 33 km altitude (Pollack *et al.* 1993). Calculations at WU used 3 ppm H_2S, based on the "preliminary" value of 3 ± 2 ppm H_2S reported by the PV mass spectrometer at altitudes below 20 km (Hoffman *et al.* 1980). The VI calculations included 0.1 ppm H_2S and 0.2 ppm S_2.

HCl and HF. These gases were included in calculations done at WU to model the kinetics of reactions using ClO and FO to convert CO to CO_2. Otherwise Cl and F do not have a noticeable influence on C–O–N–S–H thermochem-

istry in the lower atmosphere of Venus. The adopted HCl and HF mole fractions are 0.5 ppm and 5 ppb, respectively. The IR observations by Pollack *et al.* (1993) show 0.48 ± 0.12 ppm HCl at 23.5 km, and other IR observations (Connes *et al.* 1967, DeBergh *et al.* 1989, Bézard *et al.* 1993) give 0.4–0.6 ppm HCl. The observed HF abundances are 1–10 ppb (Connes *et al.* 1967; Bézard *et al.* 1990; Pollack *et al.* 1993).

MULTICOMPONENT EQUILIBRIUM CALCULATIONS

The starting compositions in Table II constrain elemental mass balance in the C–O–N–S–H system and we assume that the total amounts of C, O, N, S, and H in the gas are independent of altitude below the cloud base (at about 45 km). We also explored the sensitivity of our calculations to variations in the SO_2, H_2O, CO, OCS, and H_2S mole fractions.

Two different computer codes were used in this study. A Gibbs free energy minimization algorithm was used at VI (Zolotov 1995) and a mass balance–mass action algorithm was used at WU (Fegley and Lodders 1994). The inputs to both sets of calculations are temperature, total pressure, elemental abundances, and thermodynamic data (Gibbs free energies or equilibrium constants) for the gases included in the calculations. The codes iteratively solve for the equilibrium abundances, at a specified temperature and pressure, of the different gases considered. Van Zeggeren and Storey (1970) describe Gibbs free energy minimization codes and Fegley and Lodders (1994) describe mass balance–mass action codes.

The compounds included in the thermochemical equilibrium calculations and the thermodynamic data sources used are listed in Table III. We studied the sensitivity of the results to the thermodynamic data as follows. At WU two separate sets of calculations were done. One set used thermodynamic data from JANAF and the second set used data from the analogous compilation by the High Temperature Institute of the Russian Academy of Sciences (Gurvich *et al.* 1989–1994). At VI, the Monte-Carlo method was used (Shapkin and Sidorov 1994). One hundred different equilibrium calculations were made using Gibbs free energy values chosen from within the published uncertainty range (at 298.15 K) of Gibbs free energies for each gas. The dispersion of the calculated mole fractions of each gas gives an indication of the uncertainties due to the uncertainties in the thermodynamic data.

TABLE III
Compounds Included in the Chemical Equilibrium Calculations[a]

CO_2	S_2O[b]	HO_2[b]	F[b]
CO	O[b]	CHO	FO[b]
OCS	O_2	H_2CO	NH_3
CS_2	O_3[b]	CH_4	NO[c]
CS	H[b]	HCl[b]	NO_2[c]
N_2	H_2	Cl_2[b]	N_2O[c]
SO_2	H_2S	Cl[b]	NS[c]
S_{1-8}	HS	ClO[b]	NH_2[c]
SO	H_2O	HF[b]	HCN[c]
SO_3	OH	F_2[b]	C (graphite)

[a] Two sets of calculations were done at Washington University. One set took all data from the JANAF Tables (Chase *et al.* 1985) and the other set took all data from Gurvich *et al.* (1989–1994). The calculations at the Vernadsky Institute took thermodynamic data from the following sources: Robie and Hemingway (1995) for O_2, H_2, S_2, H_2O, SO_2, CO, CO_2; the JANAF tables (Chase *et al.* 1985) for OH, SO, CHO, H_2CO, NS, CS, CS_2, NH_2, NH_3, HCN; the 1978 JANAF supplement (Chase *et al.* 1982) for HS, Glushko *et al.* (1978–1982) for S_{3-8}, CH_4, OCS, H_2S (enthalpy and C_p data); Cox *et al.* (1989) for S, N_2, H_2S (S^o_{298}); Pankratz (1982) for SO_3, NO, NO_2, N_2O.

[b] Only included in the calculations done at Washington University.

[c] Only included in the calculations done at the Vernadsky Institute.

RESULTS OF THE EQUILIBRIUM CALCULATIONS

Gas abundances and oxygen fugacity. Figure 1 shows the abundances of major gases as a function of fO_2 at 735.3 K. These were calculated at WU using the Gurvich *et al.* thermodynamic data. Table IV lists the calculated equilibrium abundances, for gases with mole fractions above 0.02 parts per trillion (ppt), at 735.3 and 740 K. These two temperatures were used because the VIRA model (Seiff *et al.* 1986) defines 0 km as 735.3 K (6052.0 km radius), while 740 K is the temperature at the modal radius of 6051.4 km (Ford and Pettengill 1992). For reference, at the median radius of 6051.6 km the temperature is 738.4 K and at the mean radius of 6051.8 km, the temperature is 736.8 K, both of which are inside the 735–740 K range covered in Table IV.

The agreement between the calculations done at VI and at WU (taking all thermodynamic data from either JANAF or from Gurvich *et al.* (1989–1994)) is very good, and the calculated abundances generally agree within the uncertainties listed in Table IV. Figure 2 plots the calculated abundances for gases with mole fractions of 10^{-9} and above and shows that good agreement holds over the entire temperature range considered. Our results also agree with prior work (Krasnopolsky and Parshev 1979, Fegley and Treiman 1992, Zolotov 1995).

At 740 K, SO_2 remains the dominant sulfur gas (~110–130 ppm) while OCS (~16–29 ppm) and H_2S (~0.1 ppm) are less abundant. In the WU calculations, the SO_2 abundance is decreased from 130 ppm to 108 ppm by formation

TABLE IV
Chemical Equilibrium Abundances at the Surface of Venus

		740 K 95.6 bars -0.6 km			735.3 K 92.1 bars 0.0 km			
Gas		JANAF	Gurvich	Vernadsky	JANAF	Gurvich	Vernadsky	$\pm1\sigma$[b]
CO_2	%	96.5	96.5	96.5	96.5	96.5	96.5	0
N_2		3.5	3.5	3.5	3.5	3.5	3.5	0
SO_2	ppm[a]	120	108	130	120	108	129	±0.5
H_2O		33	33	30	33	33	30	±0.04
OCS		16	28	28	16	29	29	±0.6
CO		17	17	17	16	16	15	±1.4
S_2		0.21	0.20	0.23	0.22	0.21	0.24	±0.08
H_2S		0.10	0.12	0.11	0.11	0.12	0.11	±0.03
S_2O	ppb[a]	31	20	--	32	21	--	--
H_2		3.6	4.2	3.5	3.5	4.0	3.3	±0.4
S_3		0.63	0.85	0.84	0.71	0.92	0.94	±0.98
CS_2	ppt[a]	61	66	65	64	68	67	±56
SO		29	29	31	26	26	28	±8
S_4		9.0	5.2	7.0	11	6.1	8.4	±9.0
S_5		0.56	2.1	2.0	0.76	2.7	2.5	±2.6
HS		1.1	0.88	1.0	1.0	0.81	0.93	±0.21
SO_3		0.30	0.24	0.33	0.26	0.21	0.31	±0.07
S_6		0.09	0.12	0.16	0.14	0.17	0.22	±0.25
NH_3		0.02	0.02	0.02	0.02	0.02	0.02	±0.003
$\log_{10} fO_2$		-21.32	-21.35	-21.31	-21.51	-21.53	-21.49	±0.08

[a] ppm = 10^{-6}, ppb = 10^{-9}, ppt = 10^{-12}. Gases which were included in the calculations, but which are not listed, have abundances below 0.02 ppt.

[b] The calculated range of mole fractions obtained from 100 different chemical equilibrium calculations at the Vernadsky Institute using the Monte-Carlo method (see text).

of 28 ppm OCS (Gurvich data) or to 118 ppm by formation of 16 ppm OCS (JANAF data). This does not occur in the VI calculations where 28 ppm OCS was used as an input. In this case the sulfur needed to form OCS is already present in OCS and does not need to come from SO_2. The OCS abundance is also sensitive to the temperature at which chemical equilibrium is reached. More OCS is produced at lower temperatures and less is produced at higher temperatures. This trend is opposite to that deduced by Pollack *et al.* (1993) from Earth-based IR observations of OCS at higher altitudes, predicted by the kinetic models of Krasnopolsky and Pollack (1994), and predicted by gas–solid equilibrium calculations (Fegley and Treiman 1992).

The CO abundance is also sensitive to temperature (see Fig. 2). Higher temperatures lead to more CO and lower temperatures lead to less CO. Again, this trend is opposite to the CO gradient apparent from Earth-based and spacecraft observations (e.g., Von Zahn *et al.* 1983; Marov *et al.* 1989, Pollack *et al.* 1993).

The abundances of H_2S and elemental sulfur vapor are also sensitive to temperature, with lower temperatures increasing their abundances. These temperature dependent trends were used by Zolotov (1995) to conclude that gas phase thermochemical equilibrium in the 730–750 K range controls the abundances of SO_2, OCS, and CO on Venus. Our thermochemical equilibrium calculations point in the same direction.

Our calculated fO_2 values are listed in Table IV and plotted in Fig. 3. Assuming that gas phase thermochemical equilibrium is maintained, lower temperatures lead to more reducing conditions while higher temperatures lead to more oxidizing conditions. There is very good agreement between the fO_2 calculated at VI and at WU. For example, at 740 K, the calculated $\log_{10} fO_2$ values range from −21.31

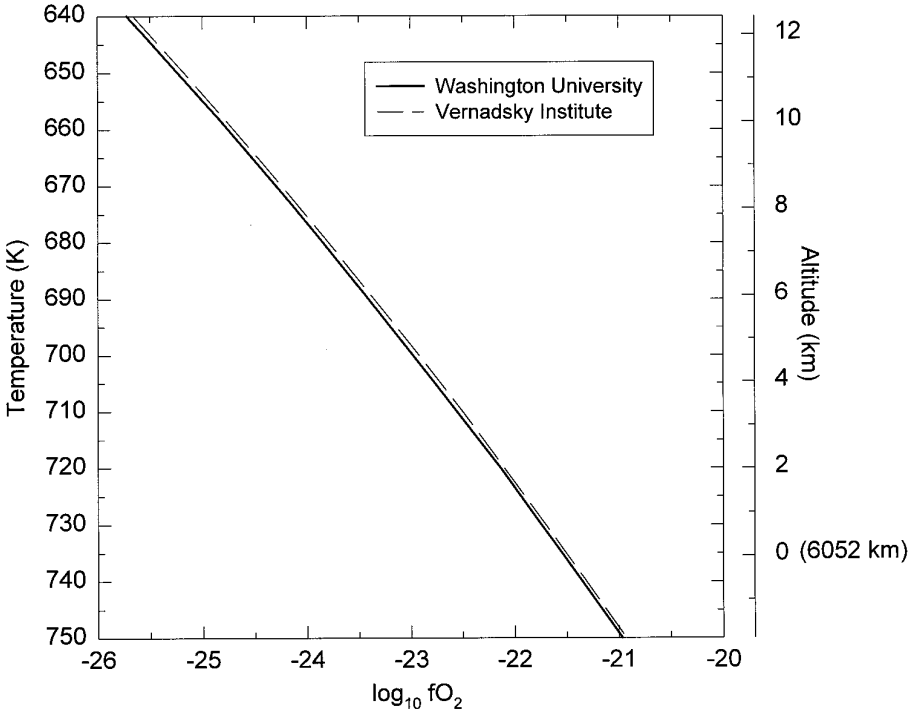

FIG. 3. The calculated oxygen fugacity (fO_2) in the lower atmosphere of Venus (solid line: Washington University calculations using data from Gurvich *et al.*; dashed line; Vernadsky Institute calculations) assuming complete gas phase chemical equilibrium as a function of temperature. The small differences between the calculations done using JANAF data and using data from Gurvich *et al.* are indistinguishable on this scale. Here and in subsequent figures, the oxygen fugacity is in bars.

to −21.35, within the dispersion of ±0.08 calculated from the Monte-Carlo calculations. The uncertainty in the thermodynamic data gives an uncertainty of only ±(0.04–0.08) in our calculated $\log_{10} fO_2$ values. Again, our results agree with prior work (e.g., Fegley and Treiman 1992, Fegley *et al.* 1996, Zolotov 1994b, 1995).

Differences between VI and WU results. The calculations at VI and WU use slightly different elemental abundances. For example, 158.5 ppm total sulfur (130 ppm SO_2 + 28 ppm OCS + 0.1 ppm H_2S + 0.2 ppm S_2) was used at VI, while 137.4 ppm total sulfur (130 ppm SO_2 + 4.4 ppm OCS + 3 ppm H_2S) was used at WU (see Table II). The two sets of calculations also have different hydrogen budgets (30 ppm total H_2 at VI versus 33 ppm total H_2 at WU).

Second, significantly different thermodynamic data for some gases also led to different results. Calculations using data from JANAF or from Gurvich *et al.* (1989–1994) gave different abundances for OCS and S_3 to S_7. Tables AI and AII in the appendix show different enthalpy and/or entropy data for OCS and S_3 to S_7 in these two compilations. Based on the detailed discussion given by Gurvich *et al.* (1989–1994), it appears that their sulfur gas data are preferable to those in JANAF or to those in the Russian edition (Glushko *et al.* 1978–1982) of the Gurvich *et al.* (1989–1994) tables. We used the Gurvich *et al.* (1989–1994) data for the rest of the calculations done at WU for this paper. However, the errors listed in Tables IV and AI show that the thermodynamic data for S_3–S_7 are very uncertain. Further experimental studies are needed to improve the data for elemental sulfur vapor.

Sensitivity tests. The data in Table II represent our best estimate for the composition of Venus' lower atmosphere, but measured trace gas abundances sometimes disagree or allow a wide range of values within the quoted uncertainties. In addition, most of the data in Table II are for altitudes >22 km and changes in gas abundances in the lower atmosphere cannot be excluded.

Our knowledge of the thermal structure of the near-surface atmosphere is also incomplete. The VIRA model of the lower 12 km uses an extrapolation below 12.5 km of data from atmospheric structure experiments on the PV and Venera 8–12 probes (Seiff *et al.* 1986). The Venera 8–10 measurements have uncertainties of ~5–8 K and ~1.5–3 bars (Avduevskiy *et al.* 1983). There are also uncertainties in extrapolating and fitting the data used in the VIRA model. In addition, Meadows and Crisp (1996) suggest that the lapse rate in the lowest 6 km of the atmosphere may be 7–7.5 K km^{-1}, instead of 8–8.2 K km^{-1} as in the VIRA model. Thus models of Venus' near-surface atmosphere may have uncertainties of 5–10 K and a few bars pressure.

The effects of variations in temperature, pressure, and gas mole fractions were studied by doing calculations at 735.3 K, the zero level in the VIRA model, using thermodynamic data from Gurvich *et al.* (1989–1994) and the WU compositional model. Each of the parameters studied was varied one at a time to assess the effect on fO_2. Varying the assumed temperature of ~735 K by ±10° leads to $\log_{10} fO_2 = -21.5 \pm 0.4$. On the other hand, varying the assumed total pressure of 92.1 bars from 89 to 95 bars leads to insignificant changes (±0.01 log units) in fO_2.

We found that fO_2 is insensitive to the amount of H_2S (3 ± 2 ppm reported by Hoffman *et al.* (1980)), with variations of only ±0.02 log units for variations of ±2 ppm in the H_2S abundance. However, fO_2 is more sensitive to variations in the abundances of other gases. For example, varying the assumed H_2O abundance from 1 to 50 ppm changes fO_2 by ~0.2 log units (−21.40 to −21.60). However, H_2O abundances below 10 ppm (corresponding to $\log_{10} fO_2 = -21.45$) seem unlikely at the surface of Venus, so the corresponding range in fO_2 may be only 0.15 log units.

Likewise, several observations give ~130 ppm SO_2, but this is uncertain by about ±30%. Varying SO_2 from 100 to 220 ppm changes $\log_{10} fO_2$ from −21.61 to −21.36. The much lower SO_2 abundances reported at 12 km by Bertaux *et al.* (1996) would lead to even lower fO_2. However, Fig. 1 shows that such low SO_2 abundances are inconsistent with the CO and OCS observations. Varying OCS from 2 to 28 ppm changes $\log_{10} fO_2$ from −21.50 to −21.68, respectively. Finally, the steep slope of the CO line in Fig. 1 shows that changes in the CO abundance have a large effect on fO_2. We later take advantage of this to constrain fO_2 at the surface of Venus.

Summary. Based on these results we conclude that our calculated fO_2 values probably have uncertainties of ±(0.4–0.5) log units from uncertainties in temperature, pressure, and gas abundances. Uncertainties in the thermodynamic data give uncertainties of ±(0.04–0.08) log units. We adopt an uncertainty of ±0.6 log units on the fO_2 values in Fig. 3 and Table IV.

THERMOCHEMICAL KINETICS

The multicomponent gas phase chemical equilibrium calculations predict fO_2 as a function of temperature, and hence altitude, in Venus' near-surface atmosphere. However, several factors suggest that chemical equilibrium may not be reached. First, gases in the near-surface atmosphere may not chemically equilibrate within a few years before convective mixing transports them upward to cooler regions (e.g., Krasnopolsky and Parshev 1979, Barsukov *et al.* 1982, Krasnopolsky and Pollack 1994, Fegley and Lodders 1995). The discrepancy between the observed and predicted gradients for OCS and CO suggests that gas phase chemical equilibrium is reached only in a thin near-surface region. Second, because OH radicals catalyze the CO → CO_2 conversion, the very small H_2O abundance in the near-surface atmosphere may prevent equilibration of CO and CO_2 (Fegley and Lodders 1995). Third, the low H_2O abundance may also prevent equilibration of other gases if OH is involved in their conversion. As a result, gas chemistry in the near-surface atmosphere may be quenched at high temperatures.

We compared the rates of six elementary gas phase reactions to the vertical mixing rate in Venus' near-surface atmosphere to test whether or not the CO → CO_2 conversion is kinetically inhibited. We also considered kinetics of elementary reactions that may convert SO_2 to OCS. The same techniques used to model the effects of vertical mixing on chemistry in the atmospheres of the outer planets (Fegley and Lodders 1994, and references therein) were used here.

The thermochemical kinetic calculations compare the chemical time constant (t_{chem}) for an elementary reaction to the physical time constant (t_{mix}) for convectively moving atmospheric gas upward to a cooler level where the elementary reaction is kinetically inhibited. The t_{chem} values are calculated from the kinetic data in Table V. The convective mixing time $t_{mix} \sim H^2/K_{eddy}$ where H is the pressure scale height (~16 km at 735 K) and K_{eddy} is the vertical eddy diffusion coefficient ($\sim 10^4$–10^6 cm^2 sec^{-1}) in Venus' near-surface atmosphere (Krasnopolsky and Parshev 1979, Barsukov *et al.* 1982, Kerzhanovich and Limaye 1986, Young *et al.* 1987). The K_{eddy} for vertical mixing in the terrestrial troposphere is about 10^4–10^5 cm^2 sec^{-1} (Warneck 1988).

At higher temperatures (lower elevations), $t_{chem} < t_{mix}$ and gas phase equilibrium is maintained. Conversely, at lower temperatures (higher elevations), reactions proceed slower, $t_{chem} > t_{mix}$, and gas phase equilibrium is not maintained. In between these two regions is a critical altitude where $t_{chem} = t_{mix}$. This quench level is different for each reaction. Once atmospheric gas rises to the quench level, reactions with sufficiently large activation energies are quenched by further vertical transport over an altitude which is small compared to the pressure scale height H.

The CO → CO_2 conversion. Photochemical modeling of CO_2 stability on Mars and Venus (McElroy and Donahue 1972, Parkinson and Hunten 1972, Yung and DeMore 1982, Nair *et al.* 1994) and thermochemical kinetic modeling of CO combustion chemistry (Warnatz 1984) indicate that one of the six elementary reactions listed in Table V could be the rate determining step for the net thermochemical conversion of CO to CO_2 (Eq. (1)). The reaction

$$CO + OH \rightarrow CO_2 + H \qquad (14)$$

TABLE V
Reactions and Rate Coefficients

Reaction	Rate Coefficient[a]	Reference
$CO + OH \rightarrow CO_2 + H$	$1.05 \times 10^{-17} T^{1.5} \exp(250/T)$	Baulch et al. 1995
$CO + SO_3 \rightarrow CO_2 + SO_2$	$1.0 \times 10^{-11} \exp(-13{,}100/T)$	Krasnopolsky & Pollack 1994
$CO + SO_2 \rightarrow CO_2 + SO$	$4.5 \times 10^{-12} \exp(-24{,}300/T)$	Mallard et al. 1994
$CO + O_2 \rightarrow CO_2 + O$	$4.2 \times 10^{-12} \exp(-24{,}000/T)$	Baulch et al. 1976
$CO + O + M \rightarrow CO_2 + M$	$1.6 \times 10^{-32} \exp(-2184/T)$	Baulch et al. 1976
$CO + ClO \rightarrow CO_2 + Cl$	$1.0 \times 10^{-12} \exp(-3700/T)$	DeMore et al. 1987
$CO + FO \rightarrow CO_2 + F$	1.25×10^{-13}	Mallard et al. 1994

[a] Reaction rate coefficients are $cm^3\ sec^{-1}$ and $cm^6\ sec^{-1}$ for two body and three body reactions, respectively.

is important for CO oxidation in flames and combustion processes (Warnatz 1984) and is a key reaction in the catalytic cycles maintaining the CO_2 atmosphere of Mars (McElroy and Donahue 1972, Parkinson and Hunten 1972). The two reactions involving CO and sulfur gases,

$$CO + SO_3 \rightarrow CO_2 + SO_2 \quad (15)$$

$$CO + SO_2 \rightarrow CO_2 + SO, \quad (16)$$

have been discussed by several authors as part of the Venus atmospheric sulfur cycle (e.g., Prinn 1985, Krasnopolsky and Pollack 1994). The other four reactions in Table V

$$CO + O_2 \rightarrow CO_2 + O \quad (17)$$

$$CO + O + M \rightarrow CO_2 + M \quad (18)$$

$$CO + ClO \rightarrow CO_2 + Cl \quad (19)$$

$$CO + FO \rightarrow CO_2 + F, \quad (20)$$

were considered to see how effectively they convert CO to CO_2 at the surface of Venus. The chemical time constant for CO oxidation by reaction (14) is given by

$$t_{chem}\ (CO) = 1/([OH]k_{14}), \quad (21)$$

where the square brackets denote molecular number densities taken from the WU chemical equilibrium calculations, and the rate constants are taken from Table V. Analogous expressions are used to calculate t_{chem} for CO oxidation via reactions (15)–(20).

Our results show that only reactions (14) to (16) are fast enough to be important in Venus' near-surface atmosphere. Reactions (17) to (20) are so slow that they are unimportant. The t_{chem} values for reactions (14)–(16) are compared to the t_{mix} values ($K_{eddy} = 10^4$–$10^6\ cm^2\ sec^{-1}$) in Figs. 4–6. The dashed lines in each figure show the effects of factor of two uncertainties in the rate constants on the t_{chem} values. Reaction (16) between CO and SO_2 is the fastest reaction and quenches at 748 ± 13 K for our nominal K_{eddy} value of $10^4\ cm^2\ sec^{-1}$ (see Fig. 4 and Table VI). The quench temperature corresponds to −1.6 ± 1.7 km (relative to 6052.0 km). Larger K_{eddy} values correspond to smaller t_{mix} values and lead to quenching at higher temperatures. However, Magellan radar altimetry shows that only about 1.5% of Venus' surface is at or below −1.6 km.

Reaction (14) between CO and OH (Fig. 5) is second fastest and quenches at 775 ± 13 K (−5.1 ± 1.7 km). Although elevations this low are observed on Venus, they cover an insignificant portion (~0.0001%) of the total surface area. There is essentially no atmospheric gas at this high temperature. The high quench temperature for this reaction is a consequence of the low H_2O concentration in the near-surface atmosphere of Venus. (The OH radicals are produced from H_2O.)

Finally, the reaction between CO and SO_3 (Fig. 6) is the third fastest and quenches at 831 ± 16 K (−12.4 ± 2.1 km). Although SO_3 is highly reactive, there is so little present in the near-surface atmosphere that oxidation of CO by SO_3 is totally negligible. Also, the quench level is well below the lowest elevations (6046.6 km radius) observed on Venus.

Reduced sulfur gas reactions with SO_2. Chemical equilibria such as reactions (3)–(5) involve O_2 and also may influence fO_2 in Venus' near-surface atmosphere (Zolotov 1995). We consider SO_2 reduction to OCS (reaction (3)), because OCS is probably the most abundant reduced sulfur gas in Venus' lower atmosphere. Reactions (4) and (5) plausibly have less influence on fO_2 because abundances

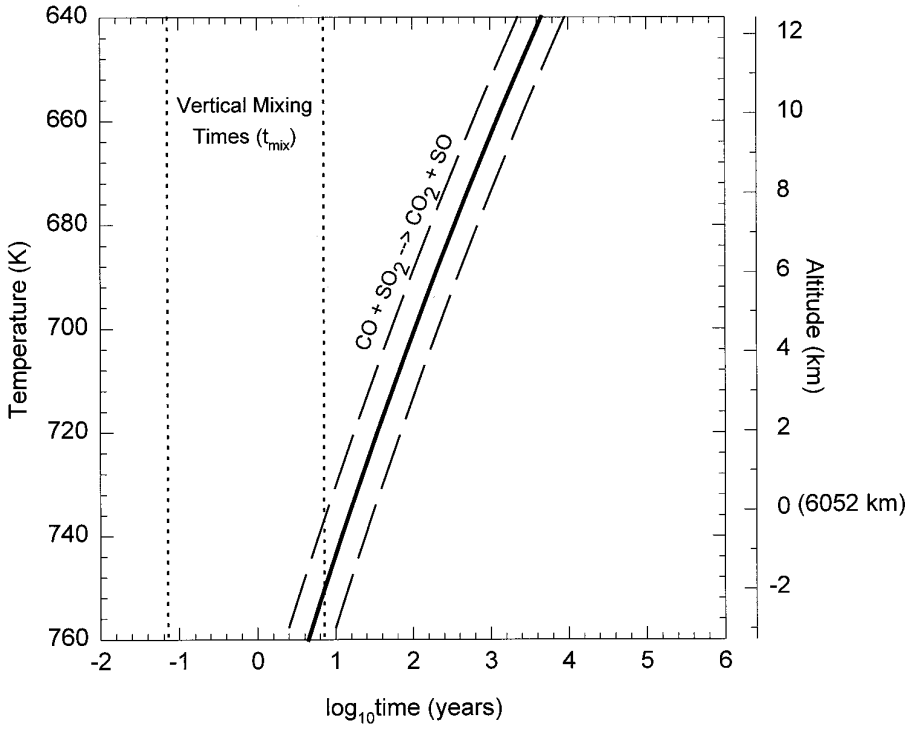

FIG. 4. A comparison of the chemical lifetime (t_{chem}) for CO oxidation by the elementary reaction CO + $SO_2 \rightarrow CO_2$ + SO with the mixing times ($t_{mix} \sim H^2/K_{eddy}$) for vertical transport in the near-surface atmosphere of Venus. The vertical dotted lines show the range of mixing times corresponding to K_{eddy} values of 10^4–10^6 cm^2 sec^{-1}. The dashed lines show the effect of a factor of two uncertainty in the rate constant on the calculated t_{chem} values. CO oxidation by this reaction is quenched at a temperature of 748 ± 13 K for our nominal K_{eddy} value of 10^4 cm^2 sec^{-1}. The quench temperature corresponds to an elevation of −1.6 ± 1.7 km. Larger values for K_{eddy} lead to smaller t_{mix} values and to higher quench temperatures. Magellan radar altimetry shows that only ~1.5% of the surface of Venus is at or below the quench level (748 K).

of H_2S and S_2 are probably lower than that of OCS. The 3 ± 2 ppm H_2S reported by Hoffman *et al.* (1980) is regarded by some as questionable (V. A. Krasnopolsky, personal communication, 1996), although Donahue and Hodges (1993) derived a similar value below 20 km.

Chemical equilibrium calculations predict that SO_2 is reduced to OCS in upwelling gas parcels on Venus. Because of the lack of good kinetic data for high temperature sulfur chemistry and uncertainties in the mechanism of the $SO_2 \rightarrow$ OCS conversion, we estimated the chemical time constant for SO_2 destruction from either reaction (16) or from the reaction

$$SO_2 + H + M \rightarrow SO + OH + M. \qquad (22)$$

We already discussed our quench calculations for reaction (16). We estimated the rate constant for reaction (22) as $k_{22} = 1.26 \times 10^{-28} \exp(-5087/T)$ cm^6 sec^{-1} from data in Mallard *et al.* (1994). The t_{chem} for SO_2 destruction via reaction (22) is

$$t_{chem}(SO_2) = 1/(k_{22}[H][M]). \qquad (23)$$

Figure 7 shows that SO_2 destruction by reaction (22) is quenched at 693 ± 9 K (5.5 ± 1.1 km) for our nominal K_{eddy} of 10^4 cm^2 sec^{-1}. However, reduction of SO or formation of the CS bond in OCS may be slower than reaction (22). The calculated quench temperature is best regarded as the lowest temperature at which SO_2 reduction to OCS proceeds in Venus' near-surface atmosphere.

Two other factors may also influence the approach to gas phase chemical equilibrium in Venus' near-surface atmosphere. The first factor is the expected increase in K_{eddy} in the planetary boundary layer due to radiative forcing, surface topography, and other factors.

Although K_{eddy} in the planetary boundary layer on Venus is probably higher than K_{eddy} in the rest of the troposphere, it is difficult to estimate the exact value. Larger K_{eddy} values closer to the surface may lead to quenching gas phase thermochemistry at slightly lower altitudes. Zolotov (1995) concluded that gas phase chemical equilibrium in the 730–750 K region of Venus' atmosphere provides the observed (or inferred) abundances of CO, SO_2, S_3, and OCS. Reactions between these gases also involve O_2, so it is plausible to suppose that the minimum equilibration temperature for reactions involving these

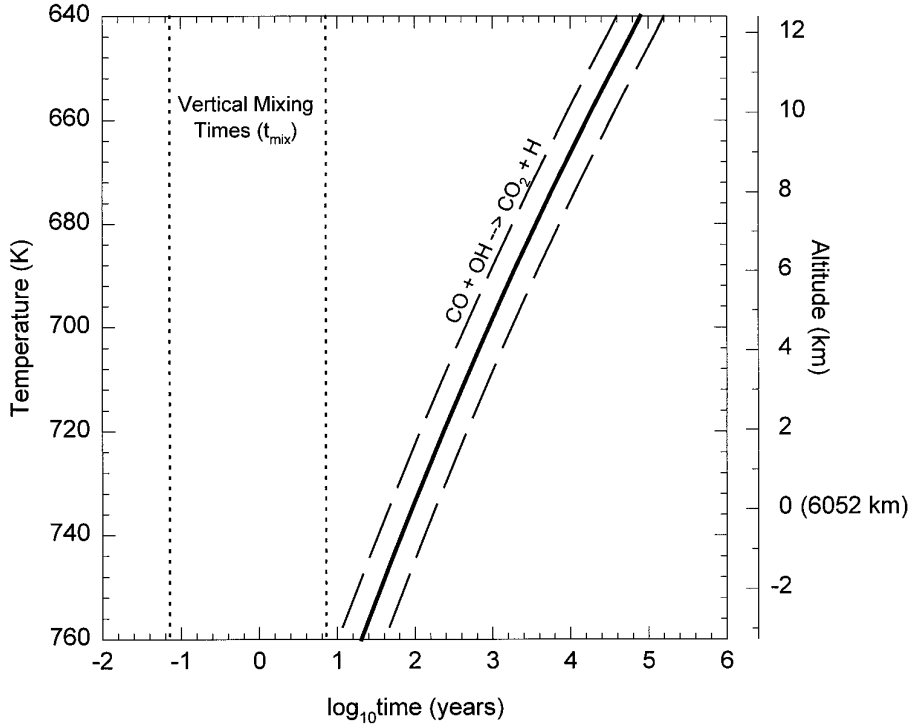

FIG. 5. A comparison of the chemical lifetime (t_{chem}) for CO oxidation by the elementary reaction CO + OH → CO_2 + H with the mixing times ($t_{mix} \sim H^2/K_{eddy}$) for vertical transport in the near-surface atmosphere of Venus. The vertical dotted lines show the range of mixing times corresponding to K_{eddy} values of 10^4–10^6 cm^2 sec^{-1}. The dashed lines show the effect of a factor of two uncertainty in the rate constant on the calculated t_{chem} values. CO oxidation by this reaction is quenched at a temperature of 775 ± 13 K (−5.1 ± 1.7 km elevation) for our nominal K_{eddy} value of 10^4 cm^2 sec^{-1}. Magellan radar altimetry shows that only ~0.0001% of the surface of Venus is at or below the quench level.

gases is also the minimum temperature at which the O_2 abundance is quenched. Zolotov (1995) found the best agreement with observed gas abundances for equilibrium at 741 K. Within uncertainties, this is identical to our calculated quench temperature of 748 ± 13 K for CO oxidation via reaction (16). Zolotov's work also suggests that our quench temperature of 693 ± 9 K for the SO_2 → OCS conversion may be too low, with quenching actually taking place at a higher temperature. Based on these results, we assume here that gas phase chemical equilibrium is plausibly quenched at 740 K, and probably quenched by 730 K in the near-surface atmosphere of Venus.

The second factor is catalysis of gas phase reactions by the rocks and soil on the surface of Venus. Although this heterogeneous catalysis is difficult to evaluate, we do not feel that surface catalyzed reactions on Venus' surface will significantly alter the results of our gas phase thermochemical kinetic calculations. In general the silicate rocks and minerals expected to be present on Venus are less efficient catalysts than platinum metal, which is used industrially as a catalyst, but not detected in the XRF analyses of Venus' surface. Second, Magellan radar altimetry measurements (Ford and Pettengill 1992) indicate that ~87% of Venus' surface is at or below the 730 K level, which we take as the lower temperature limit for gas phase thermochemistry. Even if the surface is catalyzing gas phase thermochemistry, its influence will be limited because only 13% of the surface lies above the lower temperature limit for quenching.

Implications of the equilibrium and kinetic calculations. The results of our thermochemical equilibrium and kinetic calculations lead to several important conclusions. The major conclusion is that thermochemical equilibrium controls gas phase chemistry, at least for C–O–N–S–H gases, in only the lowest few kilometers of the atmosphere of Venus.

Mueller (1964) originally proposed that the venusian atmosphere could be divided into three zones: (i) a lower zone ($T \sim 700$ K) where thermochemical equilibrium with the surface establishes the observed gas abundances, (ii) an intermediate zone ($T \sim 240$ K) of frozen thermochemical equilibria in the clouds, and (iii) an outer zone ($T > 1500$ K) in the exosphere where photochemical reactions control gas abundances. Florensky *et al.* (1978a) modified Mueller's concept and redefined the position of the three zones. They proposed that the lower thermochemical equilibrium zone extends from the surface to ~450 K (~36 km) and the intermediate zone extends from ~450 to ~300 K (~52

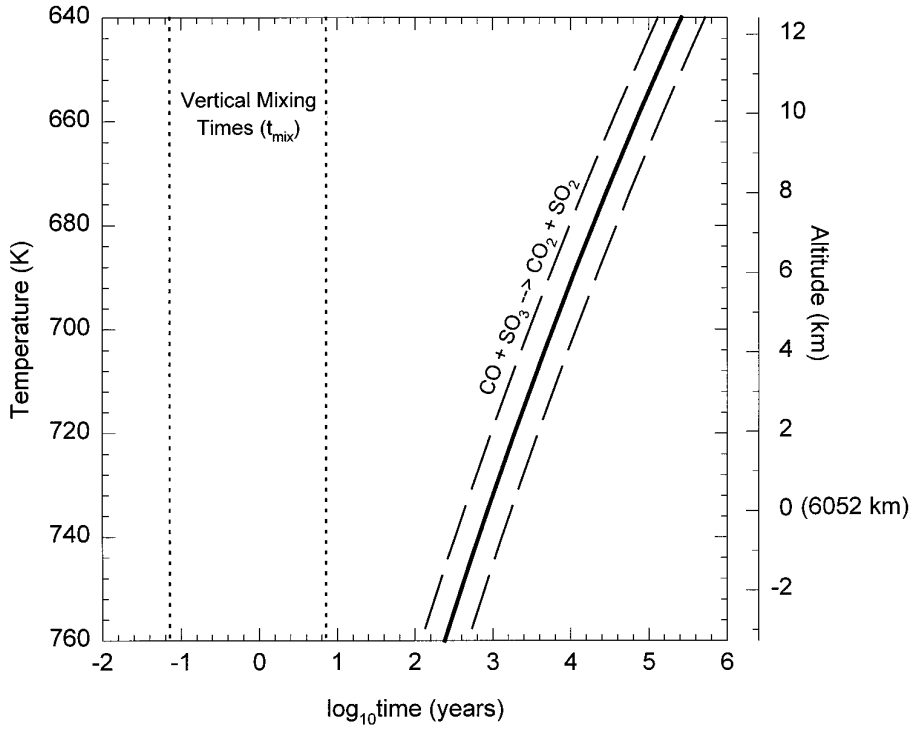

FIG. 6. A comparison of the chemical lifetime (t_{chem}) for CO oxidation by the elementary reaction CO + $SO_3 \rightarrow CO_2 + SO_2$ with the mixing times ($t_{mix} \sim H^2/K_{eddy}$) for convective motions in the near-surface atmosphere of Venus. The vertical dotted lines show the range of mixing times corresponding to K_{eddy} values of 10^4–10^6 cm^2 sec^{-1}. The dashed lines show the effect of a factor of two uncertainty in the rate constant on the calculated t_{chem} values. CO oxidation by this reaction is quenched at a temperature of 831 ± 16 K (−12.4 ± 2.1 km elevation) for our nominal K_{eddy} value of 10^4 cm^2 sec^{-1}. The lowest regions observed by Magellan radar altimetry are at −5.4 km elevation (6046.6 km radius).

km). They also proposed that the intermediate zone is a region where both thermochemical and photochemical reactions are important. Their upper photochemical zone starts at ~300 K. After the Pioneer Venus and Venera 11/12 missions, Prinn (1979) proposed that the zone of competing photochemical and thermochemical influence, at least for sulfur gases, extends even lower, perhaps reaching 10 km (~660 K).

TABLE VI
Chemical Lifetimes for CO Oxidation

	t_{chem} (years)	Quench Level[a]	
Reaction	at 0 km level	T (K)	Altitude (km)[b]
$CO + SO_2 \rightarrow CO_2 + SO$	15 (5.2-46)	748±13	-1.6±1.7
$CO + OH \rightarrow CO_2 + H$	89 (30-268)	775± 12	-5.1±1.5
$CO + SO_3 \rightarrow CO_2 + SO_2$	853 (284-2560)	831±16	-12.4±2.1

[a] For the rate constants in Table V and a nominal K_{eddy} value of 10^4 cm^2 sec^{-1}. The uncertainties and range of t_{chem} values are calculated assuming that the rate constants in Table V are uncertain by a factor of two.

[b] Relative to 6052 km radius = 0 km elevation.

The work described here and by Zolotov (1995) further restricts the purely thermochemical equilibrium zone to a thin layer very close to the surface. However, our results only apply to gas phase chemistry for C–O–N–S–H gases and do not constrain gas–solid equilibrium. Also, as emphasized by Fegley and Treiman (1992), it is likely that the HCl and HF abundances are controlled by reactions of these reactive gases with minerals on the surface.

The second conclusion is that gas phase reactions between CO, CO_2, and sulfur oxides are quenched at ~730–831 K. The quenching calculations predict that reaction (16) is the fastest reaction and that it quenches at 748 ± 13 K. The $SO_2 \rightarrow$ OCS conversion probably quenches at temperatures >693 K. Planetary boundary layer effects may increase quench temperatures while surface catalysis may decrease quench temperatures. Figure 8 shows that predicted CO concentrations range from ~25 ppm (quenching at 761 K) to ~15 ppm (quenching at 730 K). The 17 ± 1 ppm CO observed at 12 km suggests that quenching occurs closer to 730 K.

Third, our results support our earlier suggestion (Fegley *et al.* 1995b) that CO oxidation via reaction (14) is unimportant in the very dry near-surface atmosphere of Venus. There simply is not enough H_2O to produce large amounts

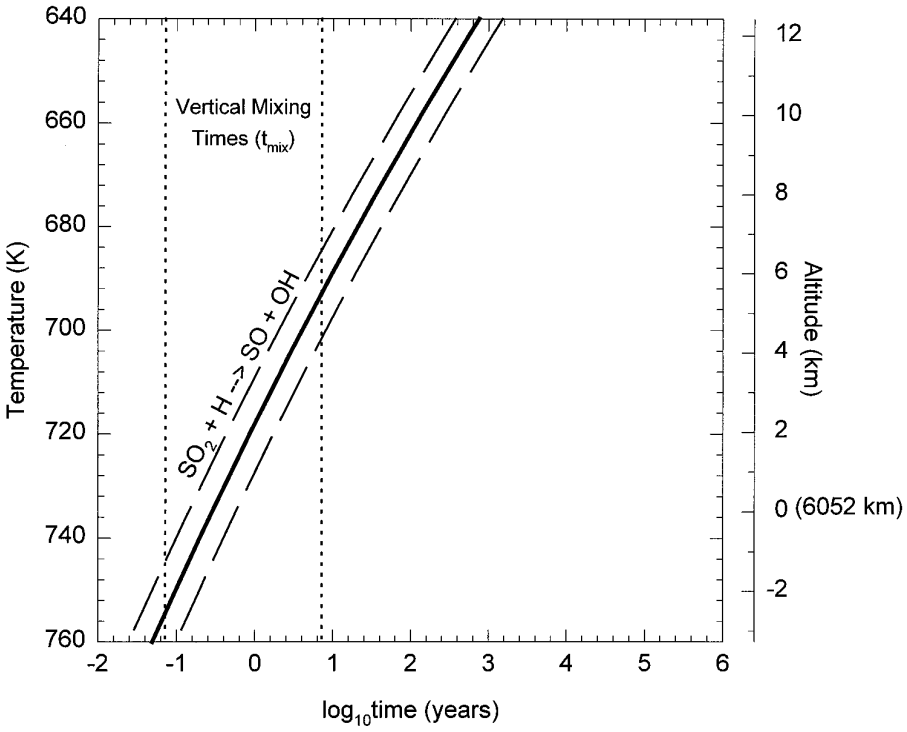

FIG. 7. A comparison of the chemical lifetime (t_{chem}) for SO_2 destruction by the elementary reaction $SO_2 + H \rightarrow SO + OH$ with the mixing times ($t_{mix} \sim H^2/K_{eddy}$) for convective motions in the near-surface atmosphere of Venus. The dashed lines show the effect of a factor of two uncertainty in the rate constant on the calculated t_{chem} values. SO_2 destruction by this reaction is quenched at 693 ± 9 K (5.5 ± 1.1 km elevation) for our nominal K_{eddy} value of 10^4 cm^2 sec^{-1}. See the text for a discussion.

of OH radicals. However, it would be interesting to study the conditions under which reaction (14) may become important.

Fourth, assuming that gas phase thermochemistry is quenched at ~730–761 K, fO_2 should also be quenched at these high temperatures (Fig. 9). Quenching reaction (16) at 730–761 K gives $fO_2 \sim 10^{-21.7}$–$10^{-20.6}$ bars. Qualitatively, as a result, rising gas parcels on Venus would become more oxidizing than they would be if they continued to equilibrate at lower temperatures. The difference between the ''equilibrium'' and ''quenched'' fO_2 increases with altitude. Eventually the rising parcels reach a critical altitude where they are more oxidizing than the MH phase boundary and hematite forms. The present calculations agree with Zolotov's (1987) suggestion that ''oxygen concentration at high altitude is equal (''frozen'') to that in the near-surface atmosphere.'' However, more detailed kinetic modeling and experimental studies are required to constrain the gas chemistry and fO_2 in the disequilibrated region of the near-surface atmosphere of Venus.

REINTERPRETATION OF THE CONTRAST EXPERIMENT

The CONTRAST experiment qualitatively measured the CO pressure at Venus' surface from the color change for reactions (12)–(13). Zolotov (1995) recalculated the thermodynamics of reaction (13) and derived $fO_2 \leq 10^{-19.7}$ bar at 740 K, corresponding to ≥2.5 ppm CO. His results are different than those reported by Florensky *et al.* (1983a,b) because they used thermodynamic data from Naumov *et al.* (1971) that did not take into account high temperature phase transitions in sodium carbonate (Na_2CO_3), sodium pyrovanadate ($Na_4V_2O_7$), and the vanadium oxides.

While continuing this work, we found significantly different $\Delta H^o_{f,298}$ values listed for $Na_4V_2O_7$ in thermodynamic data compilations (Barin 1989, Knacke *et al.* 1991, Naumov *et al.* 1971, Glushko *et al.* 1965–1983). Thus, we consulted the original papers reporting thermodynamic data for $Na_4V_2O_7$ to compile a consistent data set for this compound.

Koehler (1960) measured the enthalpy of formation ($\Delta H^o_{f,298}$) of $Na_4V_2O_7$ by acid solution calorimetry. King and Weller (1961) measured the low temperature heat capacity and calculated the entropy (S^o_{298}) of the same sample. Kubaschewski *et al.* (1981) later redetermined $\Delta H^o_{f,298}$ for $Na_4V_2O_7$ by measuring the enthalpy change for direct combination of the oxides. Their $\Delta H^o_{f,298}$ value is used by Knacke *et al.* (1991), but is about 100 kJ mol^{-1} more negative than that of Koehler (1960). However, the Kubaschewski *et al.* $\Delta H^o_{f,298}$ value appears unreliable be-

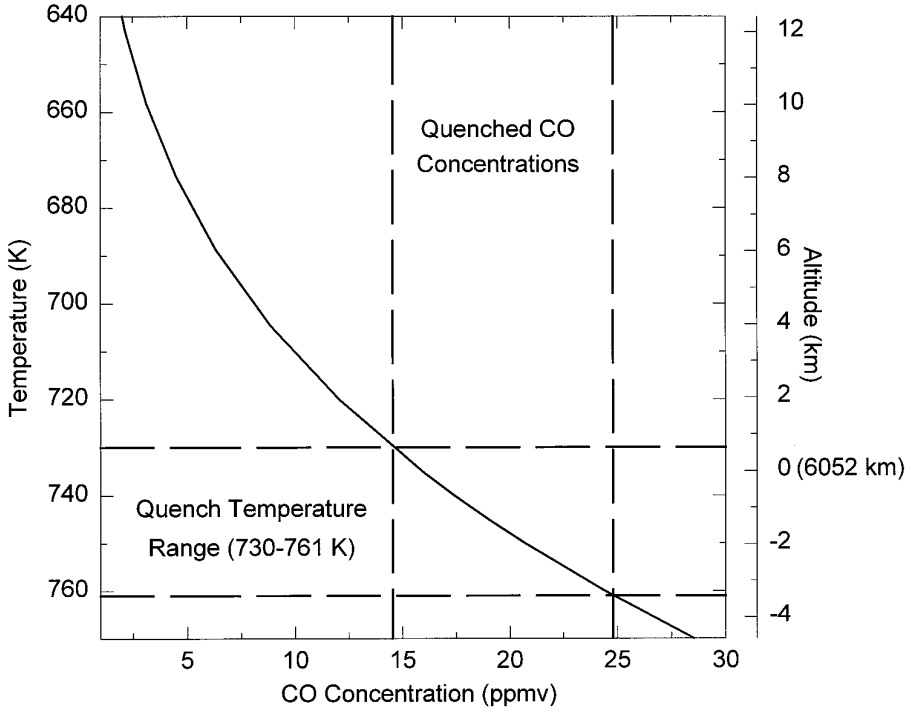

FIG. 8. A comparison of the CO concentration obtained from the chemical equilibrium calculations in Fig. 2 (solid line) with the CO concentrations predicted by quenching (vertical dashed lines) in the 730–761 K range (horizontal dashed lines). Quenching at 761 K (−3.4 km) yields 24.8 ppmv CO while quenching at 730 K (0.7 km) yields 14.5 ppmv CO. The Venera 11/12 gas chromatograph experiment observed 17 ± 1 ppmv CO at 12 km altitude (Gel'man *et al.* 1979, Marov *et al.* 1989), which is predicted to result from quenching at 739 K (−0.5 km). The Pioneer Venus gas chromatograph experiment observed 20 ± 3 ppmv CO at 22 km altitude (Oyama *et al.* 1980), which is predicted to result from quenching at 748 ± 9 K (−1.7 ± 1.2 km elevation).

cause it predicts CO equilibrium pressures >1 bar for reactions (12) and (13). Such high pressures are ruled out by laboratory studies on the use of $Na_4V_2O_7$ as a CO indicator (Florensky *et al.* 1978b).

We therefore used the calorimetric study by Koehler (1960) and updated values for necessary auxiliary data to recalculate $\Delta H^o_{f,298}$ for $Na_4V_2O_7$. Our result of -2917.8 ± 6.5 kJ mol^{-1} agrees well with the value used by Zolotov (1995). The 6.5 kJ mol^{-1} uncertainty is primarily due to an uncertainty of 6.3 kJ mol^{-1} in the $\Delta H^o_{f,298}$ of solid V_2O_5 (Chase *et al.* 1985), one of the necessary auxiliary values. We did not recalculate the S^o_{298} value of King and Weller (1961), which is used here. No high temperature enthalpy ($H^o_T - H^o_{298}$) or heat capacity (C^o_p) data have been measured for $Na_4V_2O_7$ and we used the estimated C^o_p equation of Knacke *et al.* (1991) to calculate the Gibbs free energy (ΔG^o_T) at high temperatures. Their estimated thermal functions (C^o_p, $H^o_T - H^o_{298}$, $(G^o_T - H^o_{298})/T$) are similar to those estimated by other authors at high temperatures. In general, the uncertainties introduced by estimating C^o_p at high temperatures are small (e.g., Stull and Prophet 1967, Kubaschewski and Alcock 1979). However, the unknown enthalpy of the 697 K phase transition of $Na_4V_2O_7$ and the different C^o_p of the higher temperature phase are neglected in all the estimated high temperature C^o_p equations. Neglecting the transition and the C^o_p of the higher temperature phase introduces a greater uncertainty, of a few hundred to perhaps a thousand J mol^{-1}, in the ΔG^o_T of $Na_4V_2O_7$ above 697 K.

We used our selected thermodynamic data for $Na_4V_2O_7$ in Table VII along with data from Barin (1989) to recalculate the ΔG^o values and equilibrium constants ($\Delta G^o_T = -2.303\ RT \log_{10} K$) for reactions (12) and (13) at the *P,T* conditions of the Venera 13 and Venera 14 sites (Table VIII). The equilibrium CO partial pressures for reactions (12) and (13) follow from the equations

$$\log_{10} P_{CO(12)} = -0.5 \log_{10} K_{12} \quad (24)$$

$$\log_{10} P_{CO(13)} = -\log_{10} K_{13} - \log_{10} P_{CO2}. \quad (25)$$

The results for Venera 13 and 14 are similar because the two landing sites are at about the same elevation. The nominal lower limit for CO and the nominal upper limit for fO_2 deduced from reaction (12) are ≥3.9 ppm CO ($\log_{10} fO_2 \leq -20.4$). Within the formal uncertainties of the thermodynamic data, the CO concentrations and oxygen fugacities may range from ≥2.3 ppm CO ($\log_{10} fO_2 \leq$

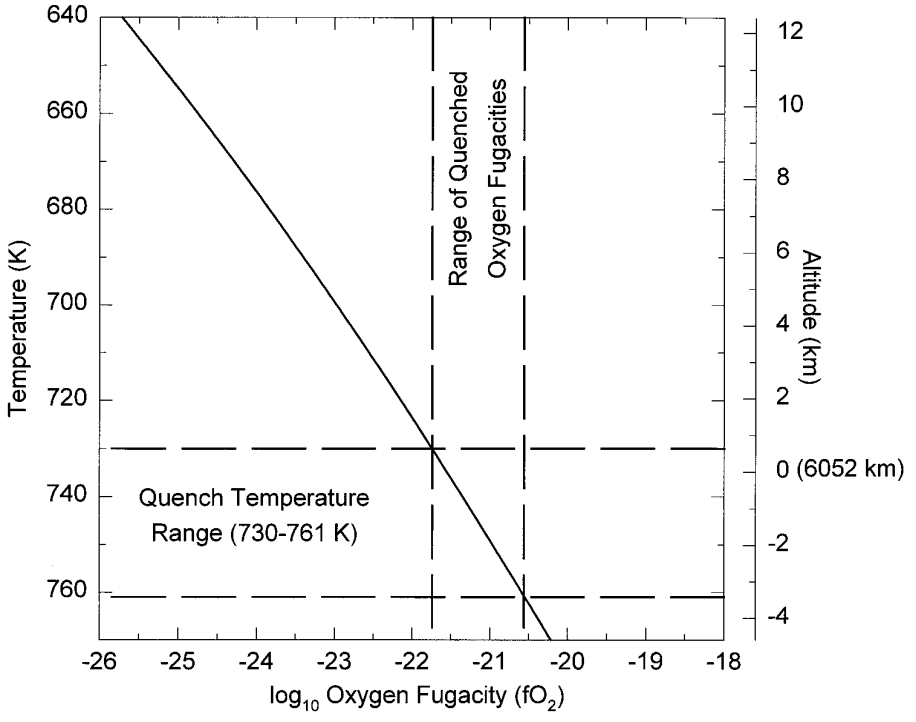

FIG. 9. A comparison of the oxygen fugacity (bars) from the chemical equilibrium calculations in Figure 3 (solid line) with the oxygen fugacity predicted by quenching (vertical dashed lines) in the 730–761 K range (horizontal dashed lines). Quenching at 761 K gives $\log_{10} fO_2 = -20.6$, while quenching at 730 K gives $\log_{10} fO_2 = -21.7$.

-20.0) to $\geq$6.8 ppm CO ($\log_{10} fO_2 \leq -20.9$). Reaction (13) yields nominal values of $\geq$1.7 ppm CO and $\log_{10} fO_2 \leq -19.7$, with values ranging from $\geq$0.6 ppm CO ($\log_{10} fO_2 \leq -18.8$) to $\geq$5.2 ppm CO ($\log_{10} fO_2 \leq -20.6$) allowed by the uncertainties in the thermodynamic data. These uncertainties and the inability to distinguish whether the observed color change of the CONTRAST indicators was due solely to reaction (12) or solely to reaction (13), or to some combination of both reactions (Florensky *et al.* 1983a,b), preclude more restrictive constraints. Despite this, the results of the CONTRAST experiment are important because they provide a lower limit on the CO concentration at the surface of Venus.

THE MAGNETITE-HEMATITE PHASE BOUNDARY

The tabulated thermodynamic data for magnetite and hematite scatter a great deal. We compared data for magnetite and hematite from several compilations (Robie and Waldbaum 1968, Spencer and Kubaschewski 1978, Kubaschewski and Alcock 1979, Robie *et al.* 1979, Chase *et al.* 1985, Ghiorso 1990, Robie and Hemingway 1995) and found that the ΔG^{o}_{T} for reaction (7) varies by tens of kilojoules mol^{-1}. Figure A1 in the appendix shows that the corresponding fO_2 varies by over three orders of magnitude at Venus surface temperatures. These large discrepancies are surprising because the thermody-

TABLE VII
Sodium Pyrovanadate ($Na_4V_2O_7$) Thermodynamic Data

Property	Value	Source
$\Delta H^{o}_{f,298}$ (kJ mol^{-1})	-2917.8 ± 6.5	Recalculated from the calorimetry by Koehler (1960)
S^{o}_{298} (J $mol^{-1}K^{-1}$)	318.4 ± 2.5	Measured by King and Weller (1961)
C^{o}_{p} (J $mol^{-1}K^{-1}$)	$323.423 + 28.87\times10^{-3}T - 5.531\times10^{6}T^{-2}$	Estimated by Knacke et al. (1991)

TABLE VIII
Results of the CONTRAST Experiments on Venera 13/14 Landers

Parameter	Venera 13	Venera 14
Latitude & Longitude[a]	-7.55°(lat), 303.69°(long)	-13.05°(lat), 310.19°(long)
Altitude above 6052 km[a]	0.2±0.3	0.3±0.3
Temperature (K)[b]	733.8±2.3	733.0±2.3
Total Pressure (Bars)[b]	91.0±1.7	90.4±1.7
ΔG°_{12} (kJ mol^{-1})[c]	-96.6±6.5	-96.8±6.5
ppm CO (reaction 12)[c]	≥4.0 (2.4-6.8)[e]	≥3.9 (2.3-6.7)[e]
$\log_{10} fO_2$ (reaction 12)[c]	≤ -20.4 (-20.0 to -20.9)	≤ -20.4 (-20.0 to -20.9)
ΔG°_{13} (kJ mol^{-1})[d]	-26.0±6.5	-26.2±6.5
ppm CO (reaction 13)[d]	≥1.8 (0.6-5.2)[e]	≥1.7 (0.6-5.0)[e]
$\log_{10} fO_2$ (reaction 13)[d]	≤ -19.7 (-18.8 to -20.6)	≤ -19.7 (-18.8 to -20.6)

[a] Positional and elevation data are taken from Table III of Fegley *et al.* (1996).
[b] Calculated from the VIRA model (Seiff *et al.* 1986).
[c] Reaction (12) is $Na_4V_2O_7 + 2CO = V_2O_3 + 2Na_2CO_3$.
[d] Reaction (13) is $Na_4V_2O_7 + CO + CO_2 = V_2O_4 + 2Na_2CO_3$.
[e] The numbers in parentheses give the range allowed by uncertainties in the thermodynamic data for reactions (12) and (13). Thus, at the Venera 13 site, reaction (13) indicates a CO mixing ratio ≥1.8 ppm, but within the uncertainties this could be ≥0.6 to ≥5.2 ppm.

namic properties of magnetite and hematite have been intensively studied and are widely believed to be well known.

As shown in Tables IX and X, these discrepancies stem from the different $\Delta H^{\circ}_{f,298}$ values chosen for magnetite and hematite in various thermodynamic data sources. The ΔG°_T of hematite up to the antiferromagnetic to paramagnetic transition at 950 K is given by

$$\Delta G^{\circ}_T(Fe_2O_3) = \Delta H^{\circ}_{f,298} + \int_{298}^{T} \Delta C^{\circ}_p \, dT - T\,\Delta S^{\circ}_{298} - T \int_{298}^{T} \frac{\Delta C^{\circ}_p}{T} \, dT, \quad (26)$$

where ΔC°_p and ΔS° are differences between reactants (Fe and O_2) and product (Fe_2O_3). An analogous equation can

TABLE IX
Hematite Thermochemical Data

$\Delta H^{\circ}_{f,298}$	S°_{298}	$C_p = a + bT + cT^{-2} + dT^2$ (J mol^{-1}K^{-1})					Source
(kJ mol^{-1})	(J mol^{-1}K^{-1})	a	b×10^{-3}	c×10^{5}	d×10^{-6}	T-Range (K)	
-825.50	87.40	128.48	-0.59	-25.90	53.32	298-950	Robie & Waldbaum (1968)
-823.41	87.45	98.28	77.82	-14.85	0	298-950	Spencer & Kubaschewski (1978)
-821.32	87.45	98.28	77.82	-14.85	0	298-950	Kubaschewski & Alcock (1979)
-824.64	87.40	186.15	-152.03	-45.35	155.35	298-950	Robie et al. (1979)
-825.50±1.3	87.40	105.54	63.81	-19.09	7.22	298-950	Chase et al. (1985)
-826.23±1.25	87.40	186.15	-152.03	-45.35	155.35	298-950	Hemingway (1990)
-822.0	87.40	158.50	-81.71	-35.47	108.91	298-955	Ghiorso (1990)
-826.2±1.3	87.4±0.2	191.20	-167.78	-46.65	168.27	298-950	Robie & Hemingway (1995) selected values for this work

TABLE X
Magnetite Thermochemical Data

$\Delta H^{o}_{f,298}$	S^{o}_{298}	$C_p = a + bT + cT^{-2} + dT^2$ (J mol^{-1}K^{-1})					Source
(kJ mol^{-1})	(J mol^{-1}K^{-1})	a	b×10^{-3}	c×10^{5}	d×10^{-6}	T-Range (K)	
-1118.8±2.1	150.75	222.91	-203.71	-33.18	325.98	298-800	Robie & Waldbaum (1968)
-1112.90	149.50	91.55	202.0	0	0	298-900	Spencer & Kubaschewski (1978)
-1116.71	151.46±2.51	91.55	201.67	0	0	298-900	Kubaschewski & Alcock (1979)
-1115.73±2.09	146.14±0.42	385.87	-619.35	-93.08	608.02	298-800	Robie et al (1979)
-1120.89±0.8	145.27	104.66	176.74	-10.04	13.05	298-900	Chase et al (1985)
-1115.73	146.14	346.24	-496.92	-82.20	506.68	298-800	Hemingway (1990)
-1117.40	146.11	321.34	-465.92	-68.21	514.49	298-848	Ghiorso (1990)
-1115.7±2.1	146.1±0.4	347.08	-499.18	-82.44	508.37	298-800	Robie & Hemingway (1995) Selected values for this work

be written for ΔG^{o}_{T} of magnetite up to the Curie point at 848 K.

Considering hematite first, the tabulated entropy and heat capacity data are essentially identical in all the literature sources. However, there is a range of ~5 kJ mol^{-1} in the selected $\Delta H^{o}_{f,298}$ values. We adopted the $\Delta H^{o}_{f,298}$ value for hematite given in Robie and Hemingway (1995). Their value is based on the work of O'Neill (1988) and Hemingway (1990), and it agrees well with the $\Delta H^{o}_{f,298}$ value selected in JANAF (Chase *et al.* 1985).

Thermodynamic data for magnetite are more uncertain. Some compilations (Robie and Waldbaum 1968, Spencer and Kubaschewski 1978, Kubaschewski and Alcock 1979) give S^{o}_{298} of 149.5 to 151.5 J mol^{-1} K^{-1}, which includes a zero point entropy of ~3.36 J mol^{-1} K^{-1}. Equilibrium studies by O'Neill (1987, 1988) and Rau (1972) of reaction (7) suggest that magnetite does not have a zero point entropy. In fact, low temperature calorimetry gives S^{o}_{298} = 146.1 J mol^{-1} K^{-1} for magnetite (Robie and Hemingway 1995). The Curie point temperature for magnetite and the C^{o}_{p} above and below the Curie point are also a matter of debate. However, the Curie point (~848 K) is above the temperature range of interest on Venus, and the tabulated C^{o}_{p} data in different compilations agree in the 298–800 K range (Table X).

The tabulated $\Delta H^{o}_{f,298}$ values for magnetite vary by ~7 kJ mol^{-1} (Table X). This is probably due to nonstoichiometry in magnetite above ~1073 K (Kubaschewski 1982). We adopt the magnetite thermodynamic data in Robie and Hemingway (1995). Their $\Delta H^{o}_{f,298}$ value is based upon the work of O'Neill (1988) and Hemingway (1990) and also agrees with the equilibrium studies by O'Neill (1987), Rau (1972), and Darken and Gurry (1945, 1946) and with the calorimetric $\Delta H^{o}_{f,298}$ value of Humphrey *et al.* (1952).

The MH phase boundary calculated from the data of Robie and Hemingway (1995) is shown in Fig. A1. A comparison of the fO_2 at the MH boundary with the calculated fO_2 at 735 K on Venus is given in Fig. 10. The gas phase fO_2 at 0 km is indistinguishable, within the uncertainties of the thermodynamic data, from the magnetite–hematite (MH) phase boundary.

Second, because of the different slopes of the MH phase boundary (Fig. A1) and the fO_2 curve for the Venus atmosphere (Fig. 3), the MH boundary intersects the gas phase curve at ~684 K (~6.6 km). In other words, hematite becomes more stable than magnetite at and above ~6.6 km elevation on the surface of Venus. Slightly different thermodynamic data for magnetite and hematite used by Zolotov (1995) gave an intersection of ~4.7 km in his calculations. The older thermodynamic data for magnetite and hematite from Robie *et al.* (1979), JANAF, and other compilations also give intersections with the gas phase fO_2 curve, but at altitudes >10 km.

Of course, these results assume complete gas phase equilibrium with decreasing temperature, but we showed earlier that gas phase thermochemistry is probably quenched by 730 K. In this case, hematite forms at lower elevations. The exact elevation at which hematite forms depends on the thermodynamic data used to calculate the MH phase boundary.

Quenching gas phase chemistry at 730 K leads to $fO_2 \sim 10^{-21.7}$ bars. Using our preferred thermodynamic data for magnetite and hematite from Robie and Hemingway (1995), hematite forms at 2.0 ± 2.0 km. On the other hand,

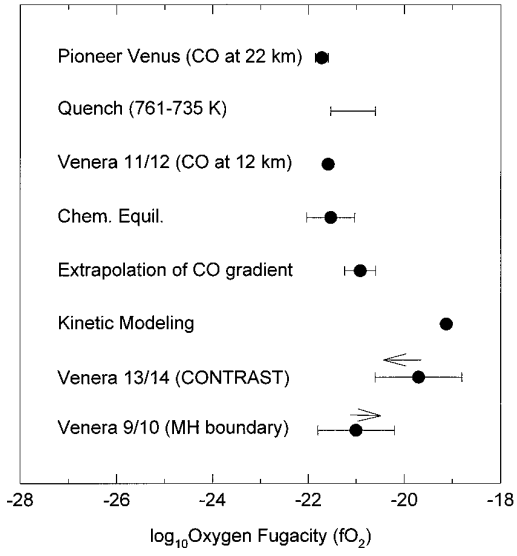

FIG. 10. A graphical summary of different estimates for the oxygen fugacity (bars) at the surface of Venus (0 km, 735.3 K level). See the caption to Fig. 11 for an explanation of the different estimates.

the data in Spencer and Kubaschewski (1978), Robie *et al.* (1979), and JANAF (Chase *et al.* 1985) predict that hematite forms at 2.7 ± 2.0, 3.6 ± 2.0, and 5.6 ± 1.5 km, respectively.

Hematite formation at lower elevations, as predicted by the Robie and Hemingway (1995) data, seems to be supported by the results of Pieters *et al.* (1986) who concluded that a high reflectance in the near-IR region apparently required Fe^{3+}-bearing minerals such as hematite at the Venera 9 and 10 landing sites. The Venera 9 site is at 0.7 ± 0.5 km elevation and the Venera 10 site is at 0.2 ± 0.6 km elevation. Within the uncertainties these sites are within the 2.0 ± 2.0 km range calculated using the Robie and Hemingway (1995) data.

SUMMARY

Figures 10 and 11 summarize different constraints on the fO_2 and CO concentration at the surface of Venus. These constraints are either observational or theoretical. We consider the observational constraints on CO first (Fig. 11). The PV gas chromatograph observed 20 ± 3 ppm CO at 22 km and the Venera 11/12 gas chromatograph observed 17 ± 1 ppm CO at 12 km. These two values are probably good upper limits for the CO concentration at 0 km on Venus because the CO concentration decreases toward the surface of Venus (e.g., Pollack *et al.* 1993). A linear fit to Earth-based and spacecraft observations of CO on Venus predicts 8.4 ± 3.0 ppm CO at 0 km (Fegley *et al.* 1996). The CONTRAST experiment on the Venera 13 and 14 landers gives a nominal lower limit of ≥1.7 ppm CO. The uncertainties on the thermodynamic data broaden this lower limit to anywhere from 0.6 to 7 ppm CO. Using the best thermodynamic data for magnetite and hematite from Robie and Hemingway (1995), the inferred presence of hematite at the Venera 9 and 10 landing sites (Pieters *et al.* 1986) corresponds to ≤8.6 ppm CO. Again, the formal uncertainties in the thermodynamic data broaden this upper limit to anywhere from 3.4 to 21.8 ppm CO. As shown in Fig. 11, the CONTRAST experiment on Venera 13/14 and the Venera 9/10 spectral reflectance data apparently bracket a narrow range of CO concentrations.

Theoretical modeling by Krasnopolsky and Pollack (1994) of the CO gradient in the atmosphere of Venus predicts 1 ppm CO at the surface. This value falls inside the range of lower limits from the CONTRAST experiment, but is otherwise lower than values from other constraints. The Krasnopolsky and Pollack model gives significantly less CO at 12 km than that observed by the Venera 11/12 gas chromatograph. However, because of a lack of kinetic data, Krasnopolsky and Pollack (1994)

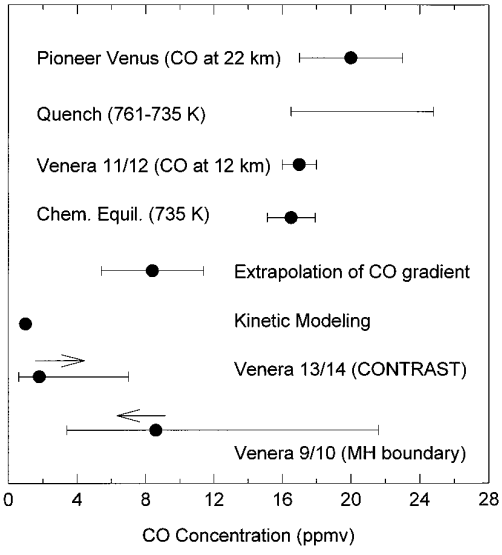

FIG. 11. A graphical summary of different estimates for the CO concentration (parts per million by volume) at the surface of Venus (0 km, 735.3 K level). The points for Pioneer Venus and Venera 11/12 are the CO concentrations (and quoted uncertainties) measured at 22 and 12 km altitude, respectively. The quench estimate is from Fig. 8. The chemical equilibrium estimate is from Table IV. The extrapolation of the CO gradient was done by Fegley *et al.* (1996). The kinetic modeling point at 1 ppmv is from the CO profile calculated by Krasnopolsky and Pollack (1994). No uncertainty was given by them. The Venera 13/14 CONTRAST experiment estimate is from Table VIII and is a lower limit to the CO concentration. The nominal lower limit as well as the uncertainty on this limit from the uncertainties in the thermodynamic data are shown. The Venera 9/10 (MH boundary) estimate shows the upper limit on the CO concentration assuming that pure hematite and pure magnetite coexist at these sites (Pieters et al 1986). The uncertainty on this upper limit is due to the uncertainties in the thermodynamic data for magnetite and hematite (Robie and Hemingway 1995).

noted that their model did not include some reactions which may be important for CO and OCS in the lowest 20 km of Venus' atmosphere.

Our chemical equilibrium calculations give 16.5 ± 1.4 ppm CO at 735 K. Quenching at 735–761 K yields ~16.5 to ~25 ppm CO. When all the observational and theoretical constraints are taken together they suggest about 3 to 20 ppm CO at 0 km on the surface of Venus.

We now consider the observational and theoretical constraints on the oxygen fugacity at the surface of Venus. The various constraints used are the same as described above for Fig. 11. Some of the fO_2 values shown in Fig. 10 are calculated from measured or inferred CO abundances by assuming 96.5% CO_2, taking the CO values from Fig. 11, and using the equation

$$\log_{10} fO_2 = 2 \log_{10} (X_{CO_2}/X_{CO}) + 9.170 - 29607.34/T. \quad (27)$$

It is important to note that the large uncertainty ranges on the upper limit from the CONTRAST experiment and on the lower limit from the Venera 9/10 spectral reflectance data come from uncertainties in the thermodynamic data for the CONTRAST reaction and the MH phase boundary. When all the observational and theoretical constraints are taken together they suggest that the fO_2 on Venus is about $10^{-21.0}$ bars. The upper limit corresponding to ~3 ppm CO is $10^{-20.0}$ bars. The lower limit corresponding to 20 ppm CO is $10^{-21.7}$ bars. These fO_2 values are indistinguishable from the MH phase boundary within the uncertainties of the thermodynamic data. We take this range of values as the "best" estimate of the fO_2 at 0 km on the surface on Venus.

Finally, this work and the chemical equilibrium calculations by Zolotov (1995) strongly suggest that despite the high surface temperature and pressure on Venus, thermochemistry prevails in only the lowest few kilometers of the atmosphere. At higher altitudes a disequilibrium region exists. In this region, the fO_2 is apparently more oxidizing than predicted by chemical equilibrium. As a result, hematite, and possibly other Fe^{3+}-bearing minerals exist on the surface. Figure 12 schematically illustrates this view of the atmosphere and surface of Venus.

SUGGESTED FUTURE WORK

We conclude by suggesting some experimental, instrumental, observational, and theoretical studies which may improve our present knowledge of the redox state of the surface and near-surface atmosphere of Venus. These topics are:

(1) Experimental studies of the fO_2 of gas mixtures with compositions relevant to the near-surface atmosphere of Venus are needed to determine the conditions under which gas phase thermochemical equilibrium is reached. Huebner (1975) showed that CO–CO_2 mixtures do not equilibrate below ~1373 K in 1 bar gas mixing furnaces, and Miyamoto and Mikouchi (1996) found that CO_2–H_2 mixtures do not equilibrate below ~1423 K in 1 bar gas mixing furnaces.

(2) Experimental studies of the stability of oxide minerals with variable composition such as titanomagnetite and hematite–ilmenite–geikielite solutions under conditions relevant to the surface of Venus. Essentially all of the existing studies have been done either in hydrothermal bombs or at temperatures much higher than those on the surface of Venus.

(3) Development of reliable oxygen fugacity and carbon monoxide sensors for use under the temperature, pressure, and composition conditions at the surface of Venus. Small sensors that could be deployed in the soil and in the atmosphere would provide key information about the role of the planetary boundary layer and surface in promoting gas phase equilibrium.

(4) The development and testing of space qualified instruments that determine (by *in situ* measurements) the mineralogy, and in particular the Fe-bearing minerals, on the surface of Venus. Laboratory studies (e.g., Vaniman *et al.* 1991, Blake *et al.* 1994, Fegley *et al.* 1995a,b, Klingelhöfer *et al.* 1995) indicate that Mössbauer spectroscopy and X-ray diffraction are suitable techniques. Based on prior spacecraft experiments, high resolution reflection spectroscopy in the visible, near-IR, and IR ranges is also suitable to identify Fe-bearing minerals present on Venus.

(5) Observational studies (Earth-based and *in situ*) of the CO, SO_2, OCS, H_2S, and S_2 abundances in the near-surface atmosphere of Venus. As illustrated in Fig. 1, the abundances of these gases are sensitive functions of the fO_2 in the near-surface atmosphere. A key feature of Fig. 1 is that low SO_2 abundances require high OCS and CO abundances and low oxygen fugacities. Such observations could confirm or refute the decreased SO_2 abundance reported by Bertaux *et al.* (1996) from UV spectroscopy on the Vega 1 and 2 spacecraft.

(6) *In situ* measurements of the thermal structure and wind field of the lower atmosphere of Venus down to the surface at several different latitudes would allow improved chemical-dynamical models of atmospheric chemistry.

(7) Theoretical models of the effects of higher water vapor abundances, such as may result from intense volcanic activity or cometary impacts, on gas phase equilibria and quenching in the near-surface atmosphere of Venus.

(8) Theoretical models of disequilibrium chemistry in the near-surface atmosphere of Venus with an emphasis on sulfur gases and the conversion of reduced and oxidized sulfur gases.

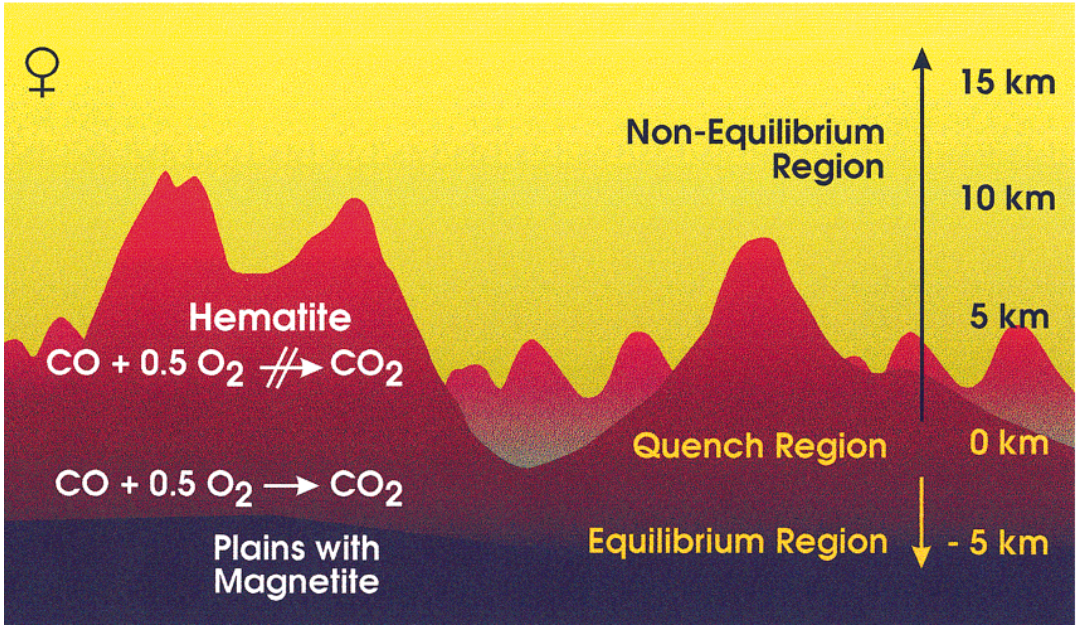

FIG. 12. A cartoon illustrating that hematite is stable over much of the surface of Venus because the quenching of the reaction CO + $0.5O_2 \rightarrow CO_2$ at low elevations (high temperatures) on the surface of Venus leads to more oxidizing conditions at higher elevations (lower temperatures). The possible presence of hematite at the Venera 9 and 10 landing sites reported by Pieters et al (1986) suggests that the magnetite → hematite conversion occurs at ~0 km elevation. This is consistent with our modeling and our selected thermodynamic data for magnetite and hematite.

APPENDIX

TABLE AI
Comparison of Thermodynamic Data (298 K) for Elemental Sulfur Vapor

Gas	JANAF Tables (Chase et al. 1985)		Gurvich et al. (1989-1994)	
	ΔH°_f (kJ mol^{-1})	S^0 (J K^{-1} mol^{-1})	ΔH°_f (kJ mol^{-1})	S^0 (J K^{-1} mol^{-1})
S	276.98±0.25	167.83±0.04	277.18±0.15	167.83±0.02
S_2	128.60±0.30	228.16±0.05	128.60±0.30	228.16±0.03
S_3	141.5±8	269.5±4	144.7±4	276.29±0.50
S_4	145.8±8	310.6±4	135.6±3	293.6±1
S_5	109.4±8	308.6±4	133.0±4	354.1±3
S_6	101.9±8	354.1±4	101.3±3	357.8±3
S_7	113.7±8	407.7±4	111.9±3.0	404.8±5
S_8	100.42±0.63	430.31±0.05	101.3±2	432.5±5

TABLE AII
Comparison of Thermodynamic Data (298 K) for Other Sulfur Gases

Gas	JANAF Tables (Chase et al. 1985)		Gurvich et al. (1989-1994)	
	ΔH°_f (kJ mol^{-1})	S^0 (J K^{-1}mol^{-1})	ΔH°_f (kJ mol^{-1})	S^0 (J K^{-1}mol^{-1})
SO	5.01±1.3	221.94±0.04	4.78±0.25	221.94±0.01
SO_2	-296.84±0.21	248.21±0.08	-296.81±0.20	248.22±0.05
SO_3	-395.8±0.7	256.8	-395.9±0.7	256.5±0.1
S_2O	-56.5±33.5	267.0	-56.0±1.4	267.0±0.2
CS	280.3±25	210.55±0.04	279.78±0.75	210.55±0.01
CS_2	116.94±0.84	237.98±0.08	116.7±1.0	237.88±0.05
OCS	-138.41±1.05	231.58	-141.7±2	231.64±0.02
HS	139.3±5.0	195.63±0.04	140.4±3.5	195.55±0.02
H_2S	-20.5±0.8	205.76	-20.6±0.5	205.80±0.05

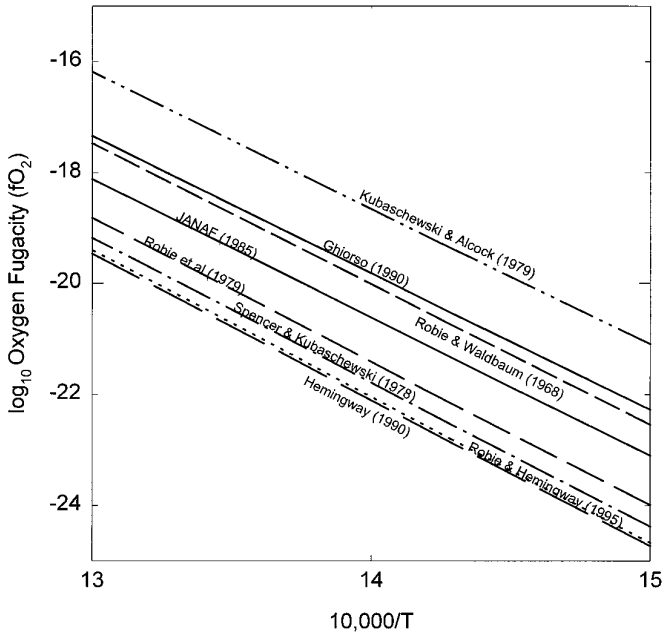

FIG. A1. A comparison of the oxygen fugacities for the magnetite–hematite phase boundary plotted as $\log_{10} fO_2$ versus $10{,}000/T$ (K). As discussed in the text, we adopt the thermodynamic data of Robie and Hemingway (1995).

ACKNOWLEDGMENTS

This work was supported by NASA Grants NAGW-2867 and NAGW-4485 and NATO Outreach CRG 960252. We thank Peter Gierasch for helpful discussions, Vladimir Krasnopolsky, and Tom Donahue for constructive reviews.

REFERENCES

Atkinson, R., D. L. Baulch, R. A. Cox, R. F. Hampson, Jr., J. A. Kerr, and J. Troe 1989. Evaluated kinetic and photochemical data for atmospheric chemistry: Supplement II. *J. Phys. Chem. Ref. Data* **18**, 881–1097.

Avduevskiy, V. S., M. Ya. Marov, Yu. N. Kulikov, V. P. Shari, A. Ya. Gorbachevskiy, G. R. Uspenskiy, and Z. P. Cheremukhina 1983. Structure and parameters of the Venus atmosphere according to Venera probe data. In *Venus* (D. M. Hunten, L. Colin, T. M. Donahue, and V. I. Moroz, Eds.), pp. 280–298. Univ. of Arizona Press, Tucson.

Barin, I. 1989. *Thermochemical Data of Pure Substances*, Vols. I and II. VCH, Weinheim, Germany.

Barsukov, V. L., V. P. Volkov, and I. L. Khodakovsky 1982. The crust of Venus: Theoretical models of chemical and mineral composition. *Proc. Lunar Planet. Sci. Conf. 13th J. Geophys. Res.* **87**, A3–A9.

Baulch, D. L., D. D. Drysdale, J. Duxbury, and S. J. Grant 1976. *Evaluated Kinetic Data for High Temperature Reactions: Homogeneous Gas Phase Reaction of the O_2–O_3 System, the CO–O_2–H Systems and of Sulphur-Containing Species*, Vol. 3. Butterworths, London.

Baulch, D. L., C. J. Cobos, R. A. Cox, P. Frank, G. Hayman, Th. Just, J. A. Kerr, T. Murrells, M. J. Pilling, J. Troe, R. W. Walker, and J. Warnatz 1995. Evaluated kinetic data for combustion modelling supplement I. *J. Phys. Chem. Ref. Data* **23**, 847–1033.

Bertaux, J. L., T. Widemann, A. Hauchecorne, V. I. Moroz, and A. P. Ekonomov 1996. Vega-1 and Vega-2 entry probes: An investigation of local UV absorption (220–400 nm) in the atmosphere of Venus (SO_2, aerosols, cloud structure). *J. Geophys. Res. Planets* **101**, 12709–12745.

Bézard, B., C. DeBergh, D. Crisp, and J. P. Maillard 1990. The deep atmosphere of Venus revealed by high-resolution nightside spectra. *Nature* **345**, 508–511.

Bézard, B., C. DeBergh, B. Fegley, Jr., J. P. Maillard, D. Crisp, T. Owen, J. B. Pollack, and D. Grinspoon 1993. The abundance of sulfur dioxide below the clouds of Venus. *Geophys. Res. Lett.* **20**, 1587–1590.

Blake, D. F., D. T. Vaniman, and D. L. Bish 1994. A mineralogical instrument for planetary applications. *Lunar Planet. Sci. XXV*, 121–122.

Chase, M. W., Jr., J. L. Curnutt, J. R. Downey, Jr., R. A. McDonald, A. N. Syverud, and E. A. Valenzuela 1982. JANAF Thermochemical Tables, 1982 Supplement. *J. Phys. Chem. Ref. Data* **11**, 695–940.

Chase, M. W., Jr., C. A. Davies, J. R. Downey, Jr., D. J. Frurip, R. A. McDonald, and A. N. Syverud 1985. *JANAF Thermochemical Tables, 3rd ed. J. Phys. Chem. Ref. Data* **14** (Suppl. 1), Am. Chem. Soc. and Am. Inst. of Phys.

Connes, P., J. Connes, W. S. Benedict, and L. D. Kaplan 1967. Traces of HCl and HF in the atmosphere of Venus. *Astrophys. J.* **147**, 1230–1237.

Connes, P., J. Connes, L. D. Kaplan, and W. S. Benedict 1968. Carbon monoxide in the Venus atmosphere. *Astrophys. J.* **152**, 731–743.

Cox, J. D., D. D. Wagman, and V. A. Medvedev 1989. *CODATA Key Values for Thermodynamics*. Hemisphere Publishing, New York.

Darken, L. S., and R. W. Gurry 1945. The system iron–oxygen. I. The wüstite field and related equilibria. *J. Am. Chem. Soc.* **67**, 1398–1412.

Darken, L. S., and R. W. Gurry 1946. The system iron–oxygen. II. Equilibrium and thermodynamics of liquid oxide and other phases. *J. Am. Chem. Soc.* **68**, 798–816.

deBergh, C., J. P. Maillard, B. Bézard, T. Owen, and B. L. Lutz 1989. Ground-based high resolution spectroscopy of Venus near 3.6 microns. *Bull. Am. Astron. Soc.* **21**, 926.

deBergh, C., B. Bézard, D. Crisp, J. P. Maillard, T. Owen, J. Pollack, and D. Grinspoon 1995. Water in the deep atmosphere of Venus from high-resolution spectra of the night side. *Adv. Space Res.* **15**, 79–88.

deMore, W. B., D. M. Golden, R. F. Hampson, C. J. Howard, M. J. Kurylo, M. J. Molina, A. R. Ravishankara, and S. P. Sander 1987. *Chemical Kinetics and Photochemical Data for Use in Stratospheric Modeling.* Evaluation 8, JPL Publication 87–41.

Donahue, T. M., and R. R. Hodges 1993. Venus methane and water. *Geophys. Res. Lett.* **20,** 591–594.

Drossart, P., B. Bézard, Th. Encrenaz, E. Lellouch, M. Roos, F. W. Taylor, A. D. Collard, S. B. Calcutt, J. Pollack, D. H. Grinspoon, R. W. Carlson, K. H. Baines, and L. W. Kamp 1993. Search for spatial variations of the H_2O abundance in the lower atmosphere of Venus from NIMS–*Galileo*. *Planet. Space Sci.* **41**, 495–504.

Ekonomov, A. P., Yu. M. Golovin, and B. E. Moshkin 1980. Visible radiation observed near the surface of Venus: Results and their interpretation. *Icarus* **41**, 65–75.

Fegley, B., Jr., and R. G. Prinn 1989. Estimation of the rate of volcanism on Venus from reaction rate measurements. *Nature* **337**, 55–58.

Fegley, B., Jr., and A. H. Treiman 1992. Chemistry of atmosphere-surface interactions on Venus and Mars. In *Venus and Mars: Atmospheres, Ionospheres, and Solar Wind Interactions* (J. G. Luhmann, M. Tatrallyay, and R. O. Pepin, Eds.), pp. 7–71. AGU, Washington, DC.

Fegley, B., Jr., and K. Lodders 1994. Chemical models of the deep atmospheres of Jupiter and Saturn. *Icarus* **110**, 117–154.

Fegley, B., Jr., and K. Lodders 1995. Chemical models of the lower atmosphere of Venus. *Bull. Am. Astron. Soc.* **27**, 1072.

FEGLEY, B., JR., K. LODDERS, A. H. TREIMAN, AND G. KLINGELHÖFER 1995a. The rate of pyrite decomposition on the surface of Venus. *Icarus* **115**, 159–180.

FEGLEY, B., JR., G. KLINGELHÖFER, R. A. BRACKETT, N. IZENBERG, D. T. KREMSER, AND K. LODDERS 1995b. Basalt oxidation and hematite formation on the surface of Venus. *Icarus* **118**, 373–383.

FEGLEY, B., JR., G. KLINGELHÖFER, K. LODDERS, AND T. WIDEMANN 1996. Geochemistry of surface–atmosphere interactions on Venus. In *Venus II* (S. W. Boucher, D. Hunten, and R. Phillips, Eds.), in press. Univ. of Arizona Press, Tucson, AZ.

FLORENSKY, C. P., V. P. VOLKOV, AND O. V. NIKOLAEVA 1978a. A geochemical model of the Venus troposphere. *Icarus* **33**, 537–553.

FLORENSKY, C. P., B. V. KOMAROV, V. P. VOLKOV, O. V. NIKOLAEVA, A. F. KUDRJASHOVA, A. S. BASHKIROVA, AND E. A. CHAIKINA 1978b. Color indicator for oxidation–reduction conditions of high-temperature gases. Soviet patent 2675712.

FLORENSKY, C. P., O. V. NIKOLAEVA, V. P. VOLKOV, A. F. KUDRYASHOVA, A. A. PRONIN, YU. M. GEEKTIN, E. A. TCHAIKINA, AND A. S. BASHKIROVA 1983a. The oxidizing–reducing conditions on the surface of Venus according to the data of the "KONTRAST" geochemical indicator on the Venera 13 and Venera 14 spacecraft. *Cosmic Res.* **21**, 278–281.

FLORENSKY, C. P., O. V. NIKOLAEVA, V. P. VOLKOV, A. F. KUDRYASHOVA, A. A. PRONIN, YU. M. GEEKTIN, E. A. TCHAIKINA, AND A. S. BASHKOROVA 1983b. Redox indicator "CONTRAST" on the surface of Venus. *Lunar Planet. Sci.* **XIV**, 203–204.

FORD, P. G., AND G. H. PETTENGILL 1992. Venus topography and kilometer-scale slopes. *J. Geophys. Res*. **97**, 13103–13114.

GEL'MAN, B. G., V. G. ZOLOTUKHIN, N. I. LAMONOV, B. V. LEVCHUK, A. N. LIPATOV, L. M. MUKHIN, D. F. NENAROKOV, V. A. ROTIN, AND B. P. OKHOTNIKOV 1979. Analysis of chemical composition of Venus atmosphere by gas chromatography on Venera 12. *Cosmic Res*. **17**, 585–589.

GHIORSO, M. S. 1990. Thermodynamics properties of hematite-ilmenite-geikielite solid solutions. *Contrib. Mineral. Petrol.* **104**, 645–667.

GHIORSO, M. S., AND R. O. SACK 1991. Thermochemistry of the oxide minerals. In *Oxide Minerals: Petrologic and Magnetic Significance* (D. H. Lindsley, Ed.), pp. 221–264. Mineralogical Society of America, Washington, D.C.

GLUSHKO, V. P., *et al.* 1965–1983. *Termicheskie Konstanty Veshchestv*. Akademiya Nauk SSSR, Moscow.

GLUSHKO, V. P., L. V. GURVICH, G. A. BERGMAN, I. V. VEITZ, V. A. MEDVEDEV, G. A. KHACHCURVZOV, V. S. YUNGMAN 1978–1982. *Thermodynamic Properties of Individual Substances*, 3rd ed., 4 vols., High Temperature Institute, Moscow.

GOLOVIN, YU. M., B. YE. MOSHKIN, AND A. P. EKONOMOV 1983. Some optical properties of the Venus surface. In *Venus* (D. M. Hunten, L. Colin, T. M. Donahue, and V. I. Moroz, Eds.), pp. 131–136, Univ. of Arizona Press, Tucson.

GURVICH, L. V., I. V. VEYTS, AND C. B. ALCOCK 1989–1994. *Thermodynamic Properties of Individual Substances*, 4th ed., 3 vols. Hemisphere Publishing, New York.

HEMINGWAY, B. S. 1990. Thermodynamic properties of bunsenite, NiO, magnetite, Fe_3O_4, and hematite, Fe_2O_3, with select comments on selected oxygen buffer reactions. *Am. Mineral.* **75**, 781–790.

HOFFMAN, J. H., R. R. HODGES, JR., T. M. DONAHUE, AND M. B. MCELROY 1980. Composition of the Venus lower atmosphere from the Pioneer Venus mass spectrometer. *J. Geophys. Res*. **85**, 7882–7890.

HOFFMAN, J. H., R. R. HODGES, JR., M. B. MCELROY, T. M. DONAHUE, AND M. KOLPIN 1979. Venus lower atmospheric composition: Preliminary results from Pioneer Venus. *Science* **203**, 800–802.

HUEBNER, J. S. 1975. Oxygen fugacity values of furnace gas mixtures. *Am. Mineral.* **60**, 815–823.

HUMPHREY, G. L., E. G. KING, AND K. K. KELLEY 1952. *Some Thermodynamic Values for Ferrous Oxide,* U.S. Bureau Mines RI 4870. U.S. GPO, Washington, DC.

KERZHANOVICH, V. V., AND S. S. LIMAYE 1986. Circulation of the atmosphere from the surface to 100 km. In *The Venus International Reference Atmosphere* (A. J. Kliore, V. I. Moroz, and G. M. Keating, Eds.), pp. 59–83, Pergamon, Oxford.

KING, E. G., AND W. W. WELLER 1961. *Low-Temperature Heat Capacities and Entropies at 298.15 K of Three Sodium Vanadates.* U.S. Bureau Mines RI 5715. U.S. GPO, Washington, DC.

KLINGELHÖFER, G., P. HELD, R. TEUCHER, F. SCHLICHTING, J. FOH, AND E. KANKELEIT 1995. Mössbauer spectroscopy in space. *Hyperfine Interact*. 95, 305–339.

KNACKE, O., O. KUBASCHEWSKI, AND K. HESSELMANN 1991. *Thermochemical Properties of Inorganic Substances*. vols. I & II, Springer-Verlag, Berlin.

KOEHLER, M. F. 1960. Heats of formation of three sodium vanadates. U.S. Bureau of Mines RI5700. U.S. GPO, Washington, DC.

KRASNOPOLSKY, V. A. 1986. *Photochemistry of the Atmospheres of Mars and Venus*. Springer-Verlag, Berlin.

KRASNOPOLSKY, V. A., AND V. A. PARSHEV 1979. Chemical composition of Venus' troposphere and cloud layer based on Venera 11, Venera 12, and Pioneer-Venus measurements. *Cosmic Res.* **17**, 630–637.

KRASNOPOLSKY, V. A., AND J. B. POLLACK 1994. H_2O-H_2SO_4 system in Venus' clouds and OCS, CO, and H_2SO_4 profiles in Venus' troposphere. *Icarus* **109**, 58–78.

KUBASCHEWSKI, O. 1982. *Iron-Binary Phase Diagrams*. Springer-Verlag, Berlin.

KUBASCHEWSKI, O., AND C. B. ALCOCK 1979. *Metallurgical Thermochemistry*, Pergamon Press, Oxford.

KUBASCHEWSKI, O., T. HOSTER, AND R. SCHLIM 1981. The heats of formation of some sodium and barium vanadates and molybdates. *Ber. Bunsenges. Phys. Chem*. **85**, 367–369.

KUIPER, G. P. 1952. Planetary atmospheres and their origin. In *Atmospheres of the Earth and Planets* (G. P. Kuiper, Ed.), pp. 306–405. Univ. of Chicago Press, Chicago.

LEWIS, J. S. 1969. Geochemistry of the volatile elements on Venus. *Icarus* **11**, 367–385.

LEWIS, J. S. 1970. Venus: Atmospheric and lithospheric composition. *Earth Planet. Sci. Lett*. **10**, 73–80.

LEWIS, J. S., AND F. A. KREIMENDAHL 1980. Oxidation state of the atmosphere and crust of Venus from Pioneer Venus results. *Icarus* **42**, 330–337.

LINDSLEY, D. H. 1991. Experimental studies of oxide minerals. In *Oxide Minerals: Petrologic and Magnetic Significance* (D. H. Lindsley, Ed.), pp. 69–106, Mineralogical Society of America, Washington, DC.

LINKIN, V. M., J. BLAMONT, S. I. DEVYATKIN, S. P. IGNATOVA, V. V. KERZHANOVICH, A. N. LIPATOV, K. MALIK, B. I. STADNYK, YA. V. SANOTSKII, P. G. STOLYARCHUK, A. V. TERTERASHVILI, G. A. FRANK, AND L. I. KHLYUSTOVA 1988. Thermal structure of the atmosphere of Venus from the results of measurements taken by landing vechicle VEGA-2. *Cosmic Res*. **25**, 501–512.

MALLARD, W. G., F. WESTLEY, J. T. HERRON, AND R. F. HAMPSON 1994. *NIST Chemical Kinetics Database*, Ver. 6.0. NIST Standard Reference Data, Gaithersburg, MD.

MAROV, M. YA., V. P. VOLKOV, YU. A. SURKOV, AND M. L. RYVKIN 1989. Lower atmosphere. In *The Planet Venus: Atmosphere, Surface,*

Interior Structure (V. L. Barsukov and V. P. Volkov, Eds.), pp. 25–67, Nauka, Moscow, USSR.

McElroy, M. B., and T. M. Donahue 1972. Stability of the martian atmosphere. *Science* **177**, 986–988.

Meadows, V. S., and D. Crisp 1996. Ground-based near-infrared observations of the Venus night side: The thermal structure and water abundance near the surface. *J. Geophys. Res. Planets* **101**, 4595–4622.

Miyamoto, M., and T. Mikouchi 1996. Platinum catalytic effect on oxygen fugacity of CO_2–H_2 gas mixtures measured with ZrO_2 sensor at 10^5 Pa from 1300 to 700° C. *Geochim. Cosmochim. Acta*. **60**, 2917–2920.

Moroz, V. I. 1981. The atmosphere of Venus. *Space Sci. Rev*. **29**, 3–127.

Mueller, R. F. 1964. A chemical model for the lower atmosphere of Venus. *Icarus* **3**, 285–298.

Mukhin, L. M., B. G. Gel'man, N. I. Lamanov, V. V. Mel'nikov, D. F. Nenarokov, B. P. Okhotnikov, V. A. Rotin, and V. N. Khokhlov 1983. Gas chromatograph analysis of the chemical composition of the atmosphere of Venus by the landers of the Venera 13 and Venera 14 spacecraft. *Cosmic Res*. **21**, 168–172.

Nair, H., M. Allen, A. D. Anbar, and Y. L. Yung 1994. A photochemical model of the martian atmosphere. *Icarus* **111**, 124–150.

Naumov, G. B., B. N. Ryzhenko, and I. L. Khodakovsky 1971. *Handbook of Thermodynamic Data.* Atomizdat, Moscow.

O'Neill, H. St. C. 1987. Quartz–fayalite–iron and quartz–fayalite–magnetite equilibria and the free energy of formation of fayalite (Fe_2SiO_4) and magnetite (Fe_3O_4). *Am. Mineral.* **72**, 67–75.

O'Neill, H. St. C. 1988. Systems Fe–O and Cu–O: Thermodynamic data for the equilibria Fe–"FeO," Fe–Fe_3O_4, "FeO"–Fe_3O_4, Fe_3O_4–Fe_2O_3, Cu–Cu_2O, and Cu_2O–CuO from emf measurements. *Am. Mineral*. **73**, 470–486.

Oyama, V. I., G. C. Carle, F. Woeller, J. B. Pollack, R. T. Reynolds, and R. A. Craig 1980. Pioneer Venus gas chromatography of the lower atmosphere of Venus. *J. Geophys. Res*. **85**, 7891–7902.

Pankratz, L. B. 1982. *Thermodynamic Properties of Elements and Oxides*, U.S. Bureau of Mines Bull. 672. U.S. GPO, Washington, DC.

Parkinson, T. M., and D. M. Hunten 1972. Spectroscopy and aeronomy of O_2 on Mars. *J. Atmos. Sci*. **29**, 1380–1390.

Pieters, C. M., J. W. Head, W. Patterson, S. Pratt, J. Garvin, V. L. Barsukov, A. T. Basilevsky, I. L. Khodakovsky, A. S. Selivanov, A. S. Panfilov, Yu. M. Gektin, and Y. M. Narayeva 1986. The color of the surface of Venus. *Science* **234**,1379–1383.

Pollack, J. B., B. Dalton, D. H. Grinspoon, R. B. Wattson, R. Freedman, D. Crisp, D. A. Allen, B. Bézard, C. DeBergh, L. Giver, Q. Ma, and R. Tipping 1993. Near-infrared light from Venus' nightside: A spectroscopic analysis. *Icarus* **103**, 1–42.

Prinn, R. G. 1979. On the possible roles of gaseous sulfur and sulfanes in the atmosphere of Venus. *Geophys. Res. Lett*. **6**, 807–810.

Prinn, R. G. 1985. The photochemistry of the atmosphere of Venus. In *The Photochemistry of Atmospheres* (J. S. Levine, Ed.), pp. 281–336. Academic Press, New York.

Rau, H. 1972. Thermodynamics of the reduction of iron oxide powders with hydrogen. *J. Chem. Thermodyn*. **4**, 57–64.

Robie, R. A., and B. S. Hemingway 1995. *Thermodynamic Properties of Minerals and Related Substances at 298.15 K and 1 Bar (10^5 Pascals) Pressure and at Higher Temperatures,* U.S. Geological Survey Bulletin 2131. U.S. GPO, Washington, DC.

Robie, R. A., and D. R. Waldbaum 1968. *Thermodynamic Properties of Minerals and Related Substances at 298.15 K (25.0° C) and One Atmosphere (1.013 Bars) Pressure and at Higher Temperatures,* U.S. Geological Survey Bulletin 1259. U.S. GPO, Washington, D.C.

Robie, R. A., B. S. Hemingway, and J. R. Fisher 1979. *Thermodynamic Properties of Minerals and Related Substances at 298.15 K and 1 Bar (10^5 Pascals) Pressure and at Higher Temperatures,* U.S. Geological Survey Bulletin 1475, reprinted with corrections. U.S. GPO, Washington, DC.

Seiff, A., J. T. Schofield, A. J. Kliore, F. W. Taylor, S. S. Limaye, H. E. Revercomb, L. A. Sromovsky, V. I. Kerzhanovich, V. I. Moroz, and M. Ya. Marov 1986. Models of the structure of the atmosphere of Venus from the surface to 100 km altitude. in *The Venus International Reference Atmosphere* (A. J. Kliore, V. I. Moroz, and G. M. Keating, Eds.), pp. 3–58, Pergamon, Oxford.

Shapkin, A. I., and Yu. I. Sidorov 1994. Probabilistic nature of calculations of chemical protoplanetary nebula. *Geochem. Intl.* **31**(9), 115–128.

Spencer, P. J., and O. Kubaschewski 1978. A thermodynamic assessment of the iron–oxygen system. *CALPHAD* **2**, 147–167.

Stull, D. R., and H. Prophet 1967. The calculation of thermodynamic properties of materials over wide temperature ranges. In *The Characterization of High Temperature Vapors* (J. L. Margrave, Ed.), pp. 359–424. Wiley, New York, NY.

Stull, D. R., and H. Prophet 1971. *JANAF Thermochemical Tables,* 2nd ed., NSRDS-NBS-37.

Trauger, J. T., and J. I. Lunine 1983. Spectroscopy of molecular oxygen in the atmospheres of Venus and Mars. *Icarus* **55**, 272–281.

Van Zeggeren, F., and S. H. Storey 1970. *The Computation of Chemical Equilibria*. Cambridge Univ. Press, Cambridge.

Vaniman, D. T., D. L., Bish, and S. J. Chipera 1991. In-situ planetary surface analyses: The potential of X-ray diffraction with simultaneous X-ray fluorescence. *Lunar Planet. Sci. XXII*, 1429–1430.

Von Zahn, U., S. Kumar, H. Niemann, and R. G. Prinn 1983. Composition of the atmosphere of Venus. In *Venus* (D. M. Hunten, L. Colin, T. M. Donahue, and V. I. Moroz, Eds.), pp. 299–430. Univ. of Arizona Press, Tucson.

Warnatz, J. 1984. Rate coefficients in the C/H/O system. in *Combustion Chemistry* (W. C. Gardiner, Jr., Ed.), pp. 197–360. Springer-Verlag, New York.

Warneck, P. 1988. *Chemistry of the Natural Atmosphere*. Academic Press, San Diego.

Young, R. E., R. L. Walterscheid, G. Schubert, A. Seiff, V. M. Linkin, and A. N. Lipatov 1987. Characteristics of gravity waves generated by surface topography on Venus: Comparison with the VEGA balloon results. *J. Atmos. Sci*. **44**, 2628–2639.

Yung, Y. L., and W. B. DeMore 1982. Photochemistry of the stratosphere of Venus: Implications for atmospheric evolution. *Icarus* **51**, 199–247.

Zolotov, M. Yu. 1987. Redox conditions on Venus surface. *Lunar Planet. Sci.* XVIII, 1134–1135.

Zolotov, M. Yu. 1994a. Phase relations in the Fe–Ti–Mg–O oxide system and hematite stability at the condition of Venus' surface. *Lunar Planet. Sci.* XXV, 1571–1572.

Zolotov, M. Yu. 1994b. Near-surface atmosphere of venus: New estimations of redox conditions based on new data. *Lunar Planet. Sci.* XXV, 1569–1570.

Zolotov, M. Yu. 1995. A model of thermochemical equilibrium in the near-surface atmosphere of Venus. *Geokhimiya* No. 11, 1551–1569. [In Russian; translated version *Geochem. Int.* **11**, 80–100]